BEHAVIOUR AND MODELLING OF COMPOSITE BEAMS AT ELEVATED TEMPERATURES - Ductility issues

RONNY BUDI DHARMA
KANG HAI TAN

Scope of Discussion

- Motivation for the research
- Experimental Investigation on Rotational Capacity
- Finite Element Analysis on Rotational Capacity
- Modelling of Moment-Rotational Relationship
- Conclusions and Recommendations

Literature Review of Concrete Properties

- Stress-Strain Relationship

Follows EC4:1.2 proposal which is regarded as the lower bound values for different test results of normal strength concrete

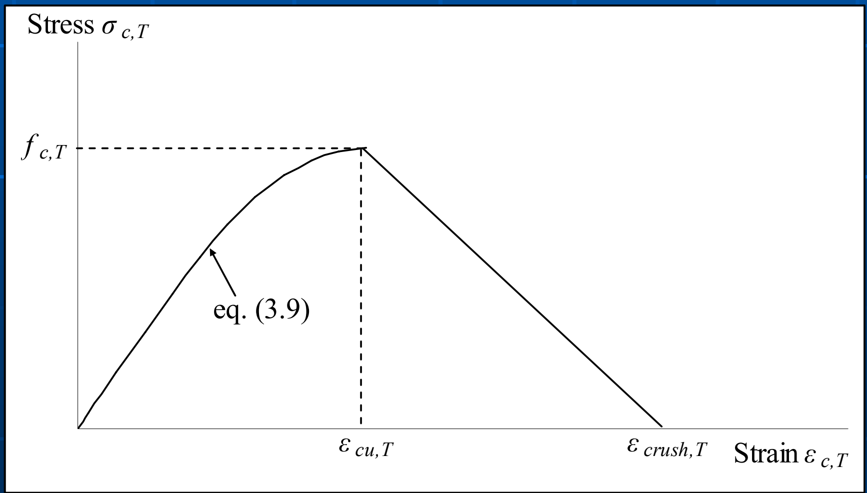

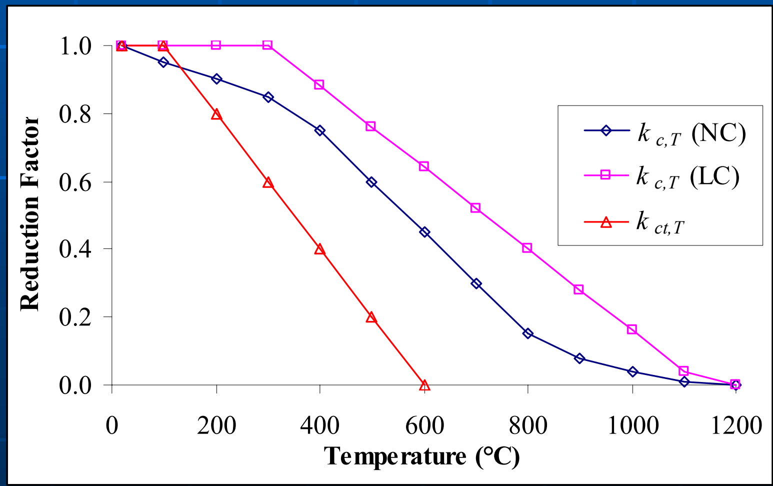

Local Buckling and Ductility

- Motivation of research
  - A considerable distortion of the cross-section in the highest moment region near to support
  - Limits the rotation capacity of beam and the degree of moment redistribution available at the support
  - May lead to premature failure
  - Has been observed in many fire incidents

Local Buckling and Ductility

- Large scale fire test in UK at Building Research Establishment (Cardington fire test) shows local buckling failure

local buckling

(compression flange and web buckling)

Local Buckling and Ductility

Local Buckling and Ductility

- 2004: Fontana and Knobloch proposed a structural model for steel plates in bending and compression at elevated temperatures

Very Limited Research on the Local Buckling and Ductility at Elevated Temperature!

Local Buckling and Ductility

- Treatment of Local Buckling
  - Current codes at ambient use the concept of cross-section behavioural classes based on ambient temperature

Limit of Width-to-Thickness Ratio				
Section Description		**EC3:1.1 (CEN, 2003)**		
		Class 1	**Class 2**	**Class 3**
Flange Outstand		9ε	10ε	14ε
Web (neutral axis at mid depth)		72ε	83ε	124ε
		Note: $\varepsilon = \sqrt{(235/p_y)}$		
Section Description		**BS5950:1-2000 (BSI, 2001)**		
		Class 1	**Class 2**	**Class 3**
Flange Outstand	**Hot Rolled**	9ε	10ε	15ε
	Welded	8ε	9ε	13ε
Web (neutral axis at mid depth)		80ε	100ε	120ε
		Note: $\varepsilon = \sqrt{(275/p_y)}$		

Shortcomings:

- Independent limitations of flange and web ratios is unreasonable
- The local ductility also depends on other factors other than width-to-thickness ratios
- The sub-division does not correspond to actual behaviour of beams

Local Buckling and Ductility

- Member behavioural classes should be used instead of cross-sectional behavioural classes
- Quantifying ductility by measuring the available inelastic rotation θ_a

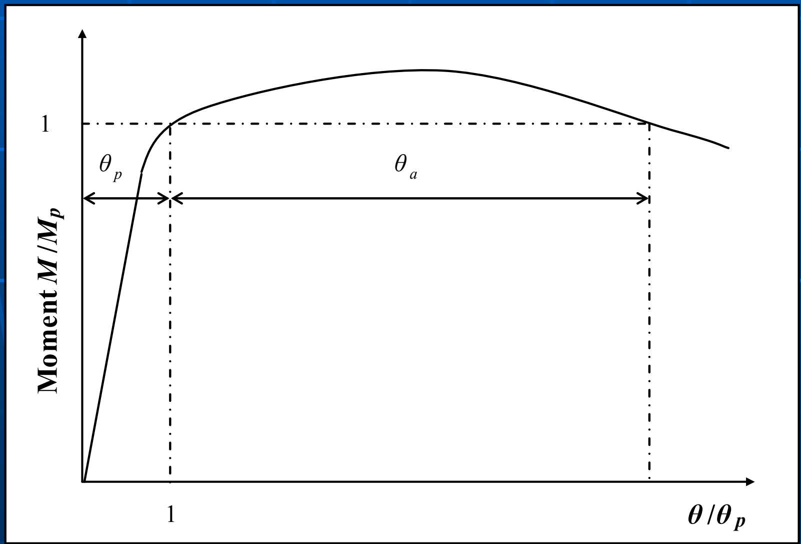

$$R_a = \theta_a / \theta_p$$

Local Buckling and Ductility

- Design codes do not address local buckling at elevated temperature
- BS5950:8 does not even provide any cross-sectional classification at elevated temperature
- EC3:1.2 classifies the cross-section as for ambient temperature design. The only modification is the introduction of reduction factor 0.85

$$\varepsilon = 0.85\sqrt{\frac{235}{p_y}}$$

- Very brief and sketchy due to lack of research and understanding
- Urgent need for better understanding of local buckling, ductility requirement and section classification at elevated temperature

Experimental Study on Rotational Capacity of Steel Beams

- Design of Specimen
  - Concept of a substitute member

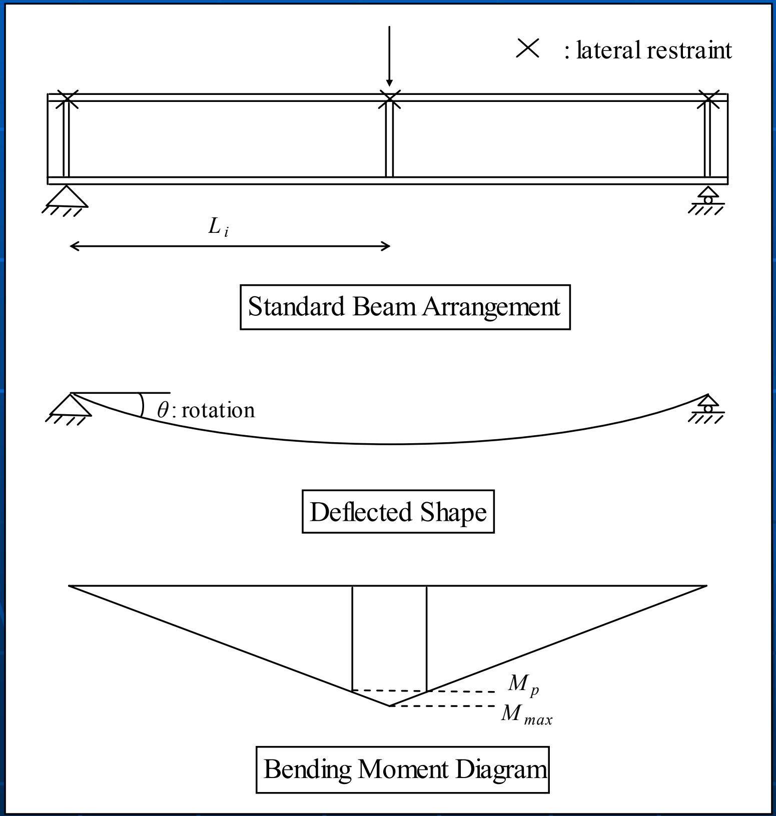

- Plastic hinge usually located at an internal support in a continuous beam
- Beam segment between the plastic hinge and adjacent point of inflection represented by each half of the simply supported beam

Experimental Investigation on Rotational Capacity

- Details of Steel Specimens

Test No.	Size	T (°C)	Coupon Type	L_E (mm)	c/t_f	d/t_w	λ_{LT} *	$M_{p,T}$ (kNm)
S1-1	305x165UB54	415	C	650	6.09	34.51	13.15	236.11
S1-2	305x165UB54	615	A	650	6.09	34.51	13.15	102.85
S2-1	305x165UB54	415	B	1725	6.09	34.51	27.30	242.86
S2-2	305x165UB54	615	B	1725	6.09	34.51	27.30	106.10
S3-1	Welded**	25	T	1725	8.15	34.51	30.06	146.67
S3-2	Welded**	415	T	605	8.15	34.51	13.45	142.67
S3-3	Welded**	615	T	605	8.15	34.51	13.45	62.33
S4-1	406x178UB54	415	E	650	8.15	47.42	13.36	410.72
S4-2	406x178UB54	615	E	650	8.15	47.42	13.36	179.43

Half-span length (L_i) = 1725mm

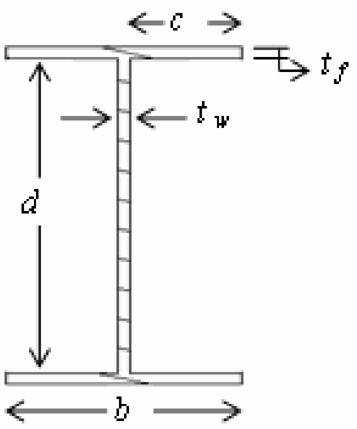

$$* \quad \lambda_{LT} = \sqrt{\frac{\pi^2 E}{f_y}}\sqrt{\frac{M_{cx}}{M_E}}$$

** b = 163mm; d = 276mm; t_f = 10mm; t_w = 8mm

- Two temperatures (415°C and 615°C)
- S3-1: ambient temperature test
- S1 and S2: effective length investigation
- S1 and S3: flange slenderness investigation
- S3 and S4: web slenderness investigation

Experimental Investigation on Rotational Capacity

- Instrumentation
  - Thermocouple

    20 locations on the steel beams surface and 2 locations measuring gas temperature

  - LVDT

    LVDT 1 - 4 measuring end rotations

    LVDT 5 - 6 measuring mid-span deflection

    LVDT 7 – 11 measuring in-plane deflection along the beam

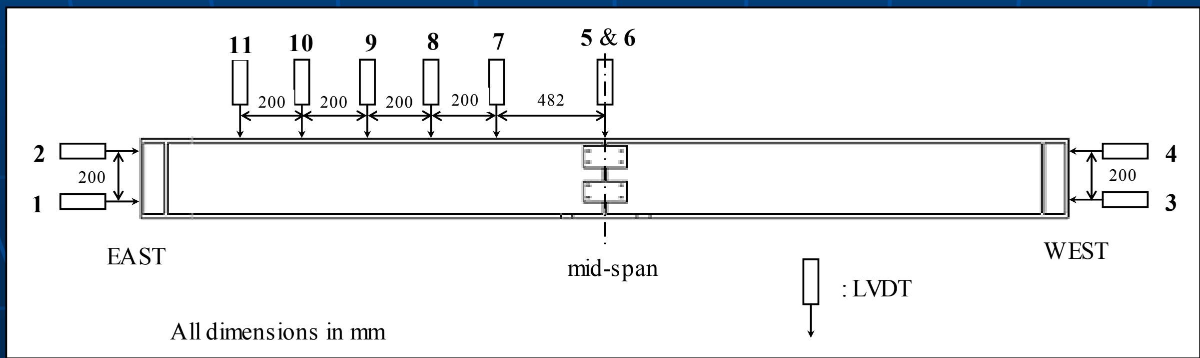

Experimental Investigation on Rotational Capacity

- Test Set-Up

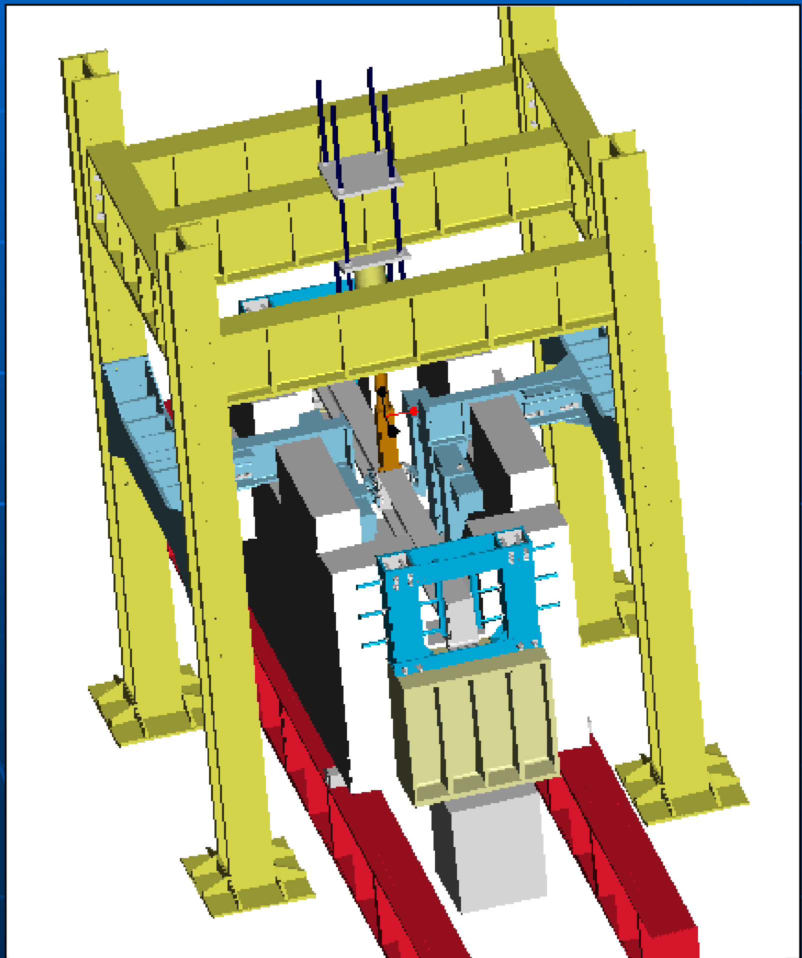

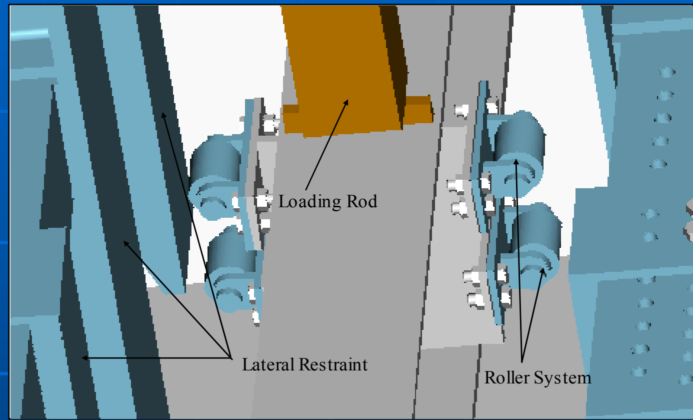

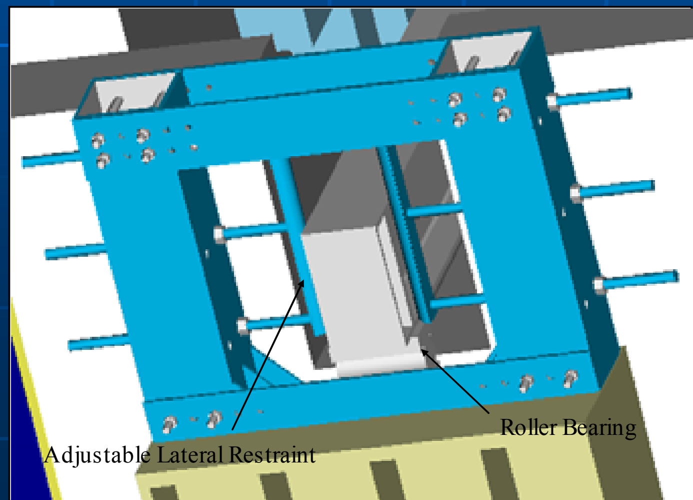

Experimental Investigation on Rotational Capacity

- Results & General Observations

Test No.	Size	T (°C)	c/t_f	d/t_w	λ_{LT}	$M_{p,T}$ (kNm)	M_m (kNm)	$M_m/M_{p,T}$	r_a	Failure Modes
S1-1	305x165UB54	415	6.09	34.51	13.15	236.11	264.70	1.121	3.73*	LB*
S1-2	305x165UB54	615	6.09	34.51	13.15	102.85	109.62	1.066	2.81*	LB*
S2-1	305x165UB54	415	6.09	34.51	27.30	242.86	262.55	1.081	1.60	LTB
S2-2	305x165UB54	615	6.09	34.51	27.30	106.10	112.04	1.056	0.93	LTB
S3-1	Welded	25	8.15	34.51	30.06	146.67	194.41	1.325	7.57	LB-LTB
S3-2	Welded	415	8.15	34.51	13.45	142.67	156.29	1.095	2.28	LB
S3-3	Welded	615	8.15	34.51	13.45	62.33	68.48	1.099	1.11	LB
S4-1	406x178UB54	415	8.15	47.42	13.36	410.72	451.26	1.099	0.68	LB
S4-2	406x178UB54	615	8.15	47.42	13.36	179.43	186.04	1.037	0.30	LB

Note: * Estimated based on numerical simulation
LB : local buckling
LTB: lateral torsional buckling
LB-LTB: local buckling followed by lateral torsional buckling

Experimental Investigation on Rotational Capacity

- Results & General Observations
  - No local and global buckling took place before the plastic moment capacity was reached – design of specimens is indeed successful!!!
  - Beams tested at 615° C deviated from linearity at an earlier stage compared with those tested at 415° C
  - After attaining plastic moment capacity, the beam deflection and rotation started to increase rapidly
  - No sudden failure
  - Two failure modes observed: local buckling of the beam flange and web near to mid-span and global buckling

Experimental Investigation on Rotational Capacity

- Results & General Observations

- Local buckling with anti-symmetric mode at equi-distance from the restrained mid-span
- Web buckling less obvious than flange buckling

- Global buckling with lateral movement mostly near mid-span
- Due to spread of yielding (different from elastic LTB)

Experimental Investigation on Rotational Capacity

- Temperature Effects

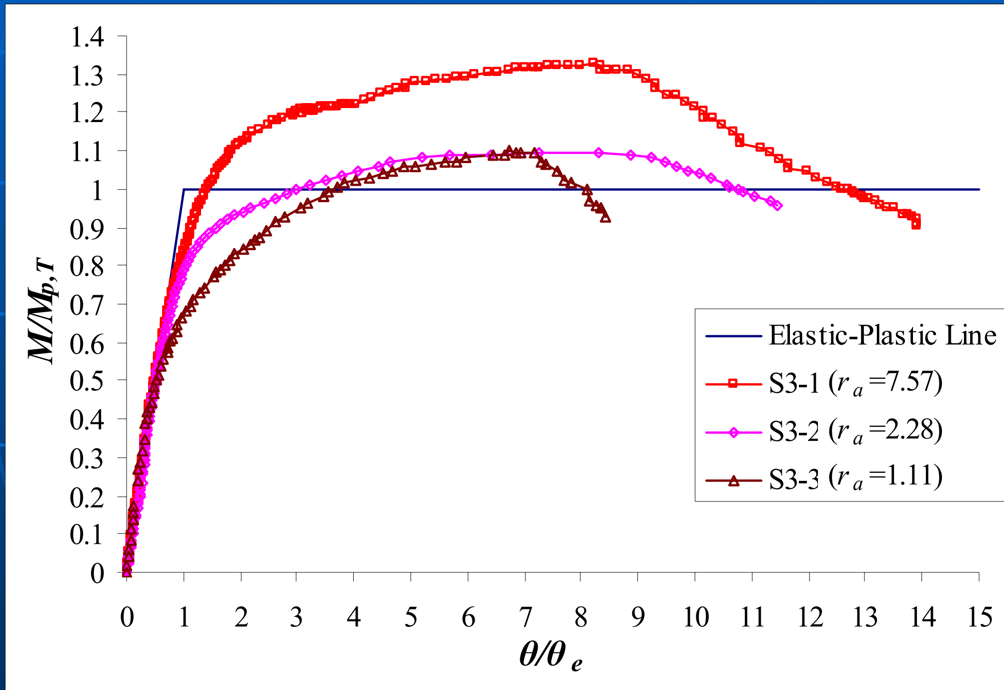

Conservatism of design plastic moment capacity has reduced from up to 30% to a low of 10% as temperature increased to 615°

- Ambient (S3-1): considerable rotational capacity (r_a = 7.57) and maximum moment of 33% above its theoretical value
- 415° C (S3-2): moment-rotation curve became non-linear and the rotational capacity reduced to 2.28 even with additional lateral restraints
- 615° C (S3-3): rotational capacity further reduced to 1.11

Experimental Investigation on Rotational Capacity

- Flange Slenderness Effects

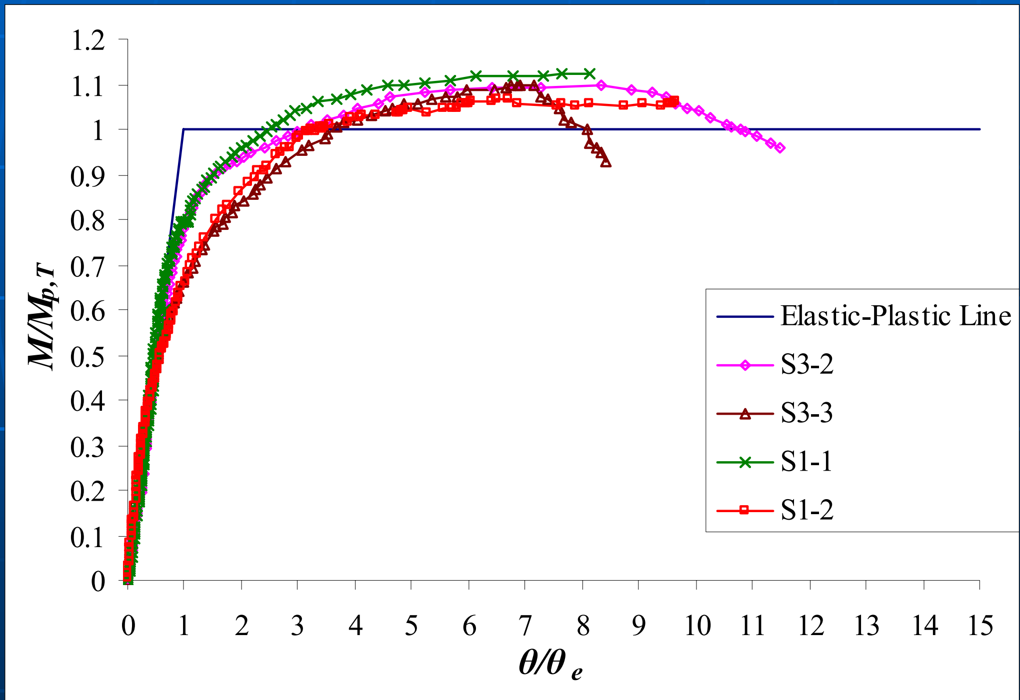

- S1-1 & S1-2: stockier flanges (6.09) than S3-2 & S3-3 (8.15), hence greater rotational capacity
- S1 test series had to be stopped due to excessive deflection
- The estimated rotational capacities of S1-1 & S1-2 were 3.73 and 2.81
- Rotational capacities of S3-2 and S3-3 are 2.28 and 1.11

Experimental Investigation on Steel Beams' Rotational Capacity

- Web Slenderness Effects

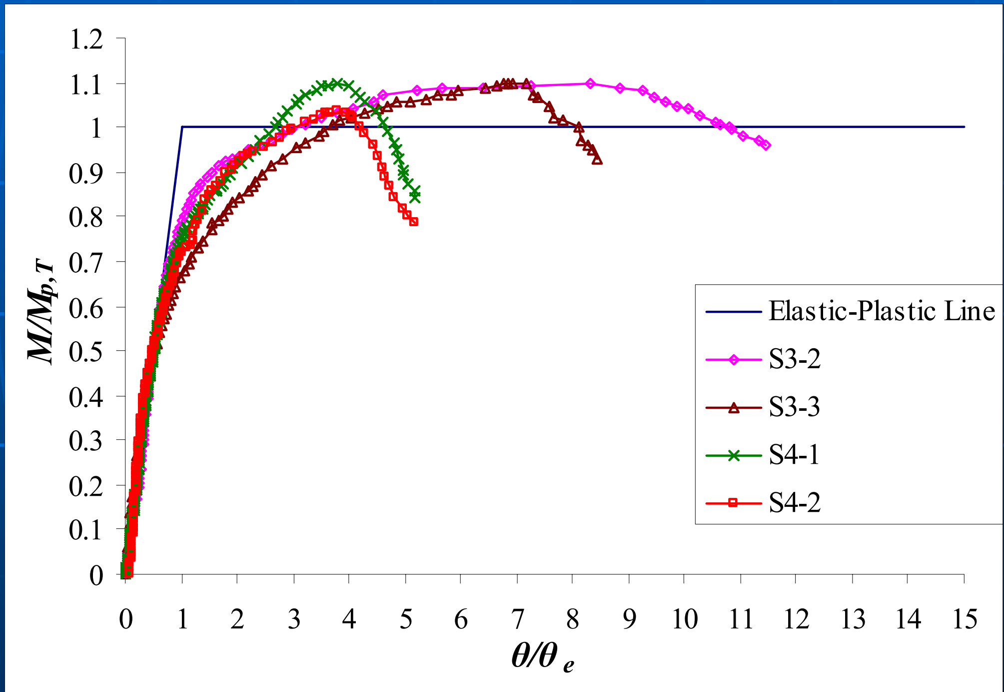

- S4-1 & S4-2 provided less rotational capacity than S3-2 & S3-3, respectively, because they have more slender webs
- S4-2 (615° C) merely reached its plastic moment capacity
- Higher grade of steel (S355) used in S4 series may also contribute to less ductility
- The stockier the web, the greater the restraints it provided against flange buckling, thus enhancing the ductility

Even though flanges are the primary elements of flexural resistance in I-sections, the web slenderness effect is also dominant.

Experimental Investigation on Steel Beams' Rotational Capacity

- Effective Length Effects

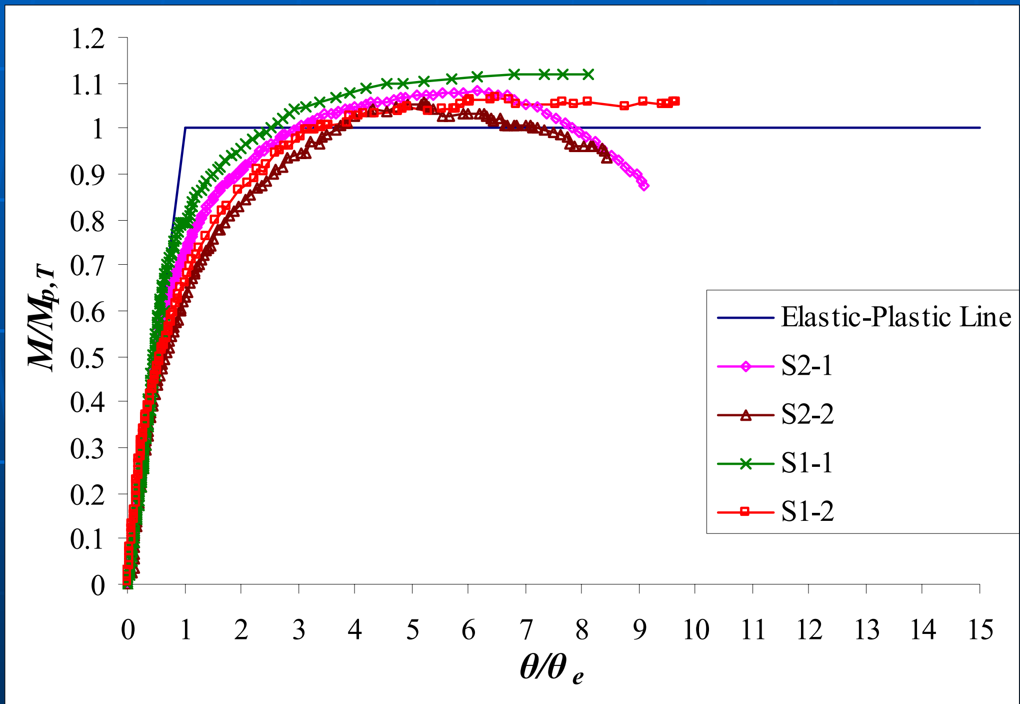

- Additional lateral restraints are provided for S1 series (effective length becomes 650 mm)
- Effective length for S2 series is 1725 mm
- A slight increase in the maximum moment was observed when effective length was reduced
- Failure mode changed from global buckling for S2 series to local buckling for S1 series

Ductility of beams is influenced not only by conventional flange and web slenderness parameters, but also by effective length which is one of the factors governing LTB

Experimental Investigation on Composite Beams

- Design of Specimen
  - Similar to steel beams (a simply supported beam subjected to a central point load)

➢The composite beam is inverted such that the decking slab is located on the underside of the steel beam and is subjected to tensile force when vertical load applied from the top

➢Length of concrete slab is kept at only 2100 mm

➢Holorib S350 (0.9 mm thick) re-entrant steel decking

➢Shear studs were connected to the steel beams and steel decking by through-deck welding

Experimental Investigation on Composite Beams

- Design of Specimen
  - After concrete curing, double layer of fire protection material consisted of 25 mm thick vermiculite and 30 mm thick ceramic blanket applied to exposed surface of concrete

Test No.	Structural Steel	Reinforcement	No. of Stud	Stud spacing (mm)	L_E (mm)	t_c (mm)
C1	305x165UB54	4-T10	8	280	563	130
C2	305x165UB54	4-T10	4	650	563	130
C3	305x127UB37	5-T10	10	220	563	130
C4	254x102UB25	5-T10	6	380	469	120
Half-span length (L_i) =			1725 mm			
Slab size (length x width) =			2100 mm x 450 mm			
Reinforcement distance to steel decking =			100 mm			
Anti-crack reinforcement =			T8 at 200 mm spacing			
Shear stud connector =			19 mm dia. x 100 mm length			

Note: 4-T10 indicates four bars of type T reinforcement with 10 mm diameter.

Experimental Investigation on Composite Beams

- Push-Out Test (Shear Studs)

  Average maximum shear strength was 115 kN per connector

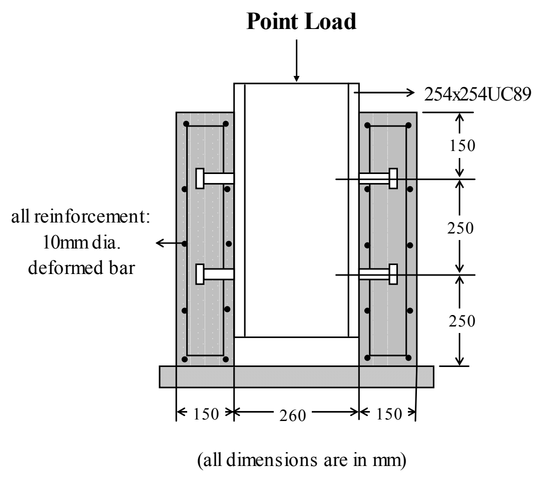

Push-Out Specimen Configuration

Push-Out Test Set-Up

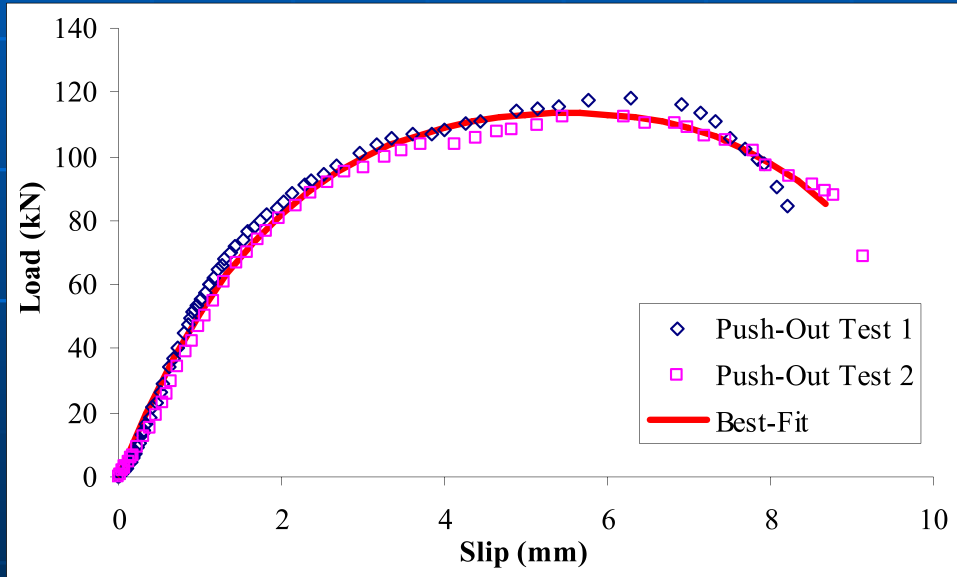

Experimental Investigation on Composite Beams

- Temperature Developments

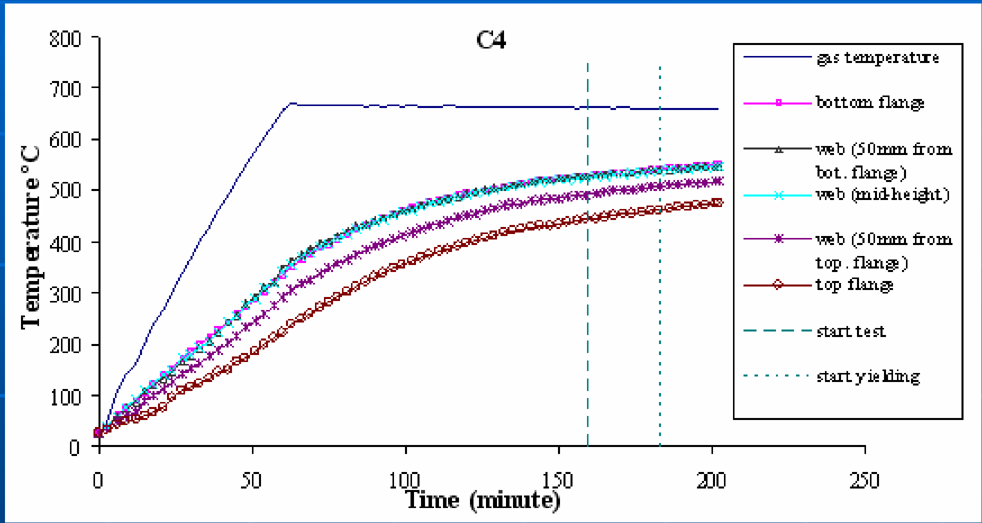

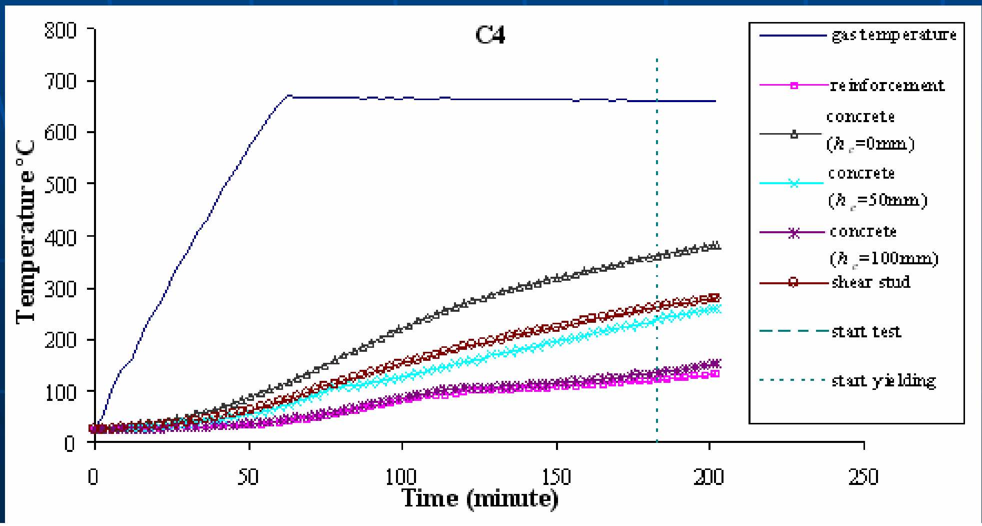

➢Furnace temperature set between 650 and 800° C based on 7 to 10° C/min

➢Temp of rebar (100 mm above top flange) and concrete (h_c = 100 mm) was very close

➢Shear stud temperature was in between the recorded concrete temperature closest to top flange (h_c = 0 mm) and h_c = 50 mm

Experimental Investigation on Composite Beams

- Temperature Developments

Thermocouple Location	C1 Test	C2 Test	C3 Test	C4 Test	Average
bottom flange	1.00	1.00	1.00	1.00	1.00
web (50 mm above bottom flange)	1.02	1.01	1.01	1.00	1.01
web (mid-height)	1.02	1.00	1.00	0.99	1.00
web (50 mm below top flange)	0.97	0.96	0.93	0.94	0.95
top flange	0.90	0.87	0.83	0.85	0.86
concrete (directly above top flange)	0.65	0.39	0.54	0.61	0.55
concrete (50 mm above top flange)	0.36	0.24	0.33	0.38	0.33
concrete (100 mm above top flange)	0.26	0.17	0.22	0.22	0.22
reinforcement	0.18	0.17	0.20	0.22	0.19
shear stud	0.51	0.42	0.37	0.48	0.44

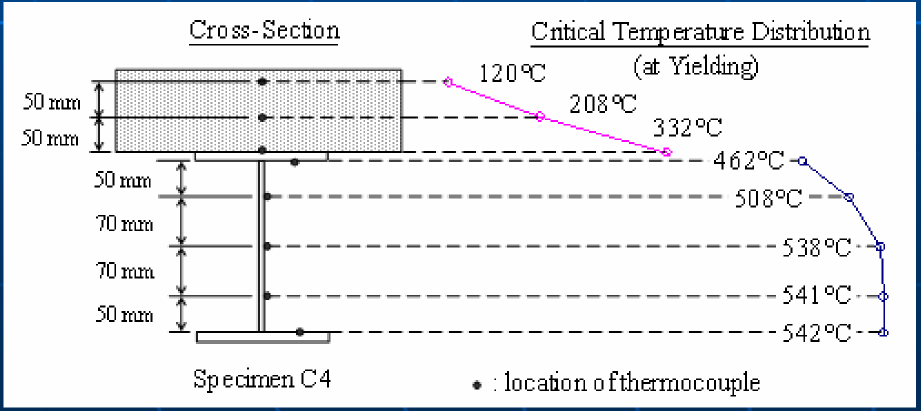

- Average top flange temperature around 0.86 of bottom flange temperature due to the heat sink and shielding effect of concrete slab
- Web temperature varied parabolically between the top and bottom flange temperatures
- Temperature profile of concrete seemed to be parabolic as well
- The maximum temperature of the shear stud connector for all beams was 340° C

Experimental Investigation on Composite Beams

- General Observations

Test No.	$M_{p,T}$ (kNm)	M_m (kNm)	$M_m/M_{p,T}$	θ_p/θ_e	θ_u/θ_e	r_a
C1	133.89	146.05	1.091	1.783	5.544	2.11
C2	155.33	183.79	1.183	2.067	5.879	1.84
C3	177.62	200.70	1.130	1.860	5.306	1.85
C4	105.19	116.01	1.103	1.910	3.829	1.00

- All specimens reached their respective plastic moment capacity at a rotation of 1.78 to 2.07 of their respective elastic rotation
- The maximum plastic moment for all specimens tested at elevated temperatures is around 110% of its theoretical value, except C2 specimen
- C1 specimen has the greatest rotational capacity of 2.11, while C4 specimen has the lowest rotational capacity of only 1.00

Experimental Investigation on Composite Beams

- General Observations

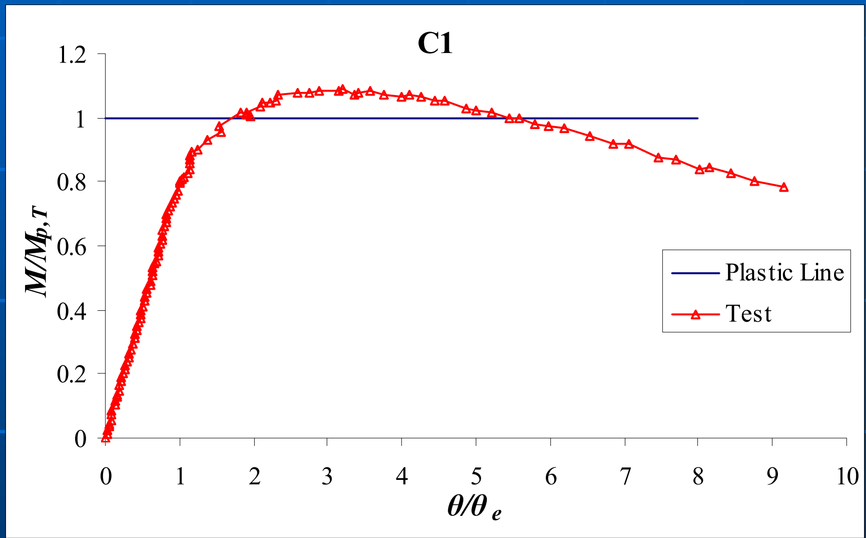

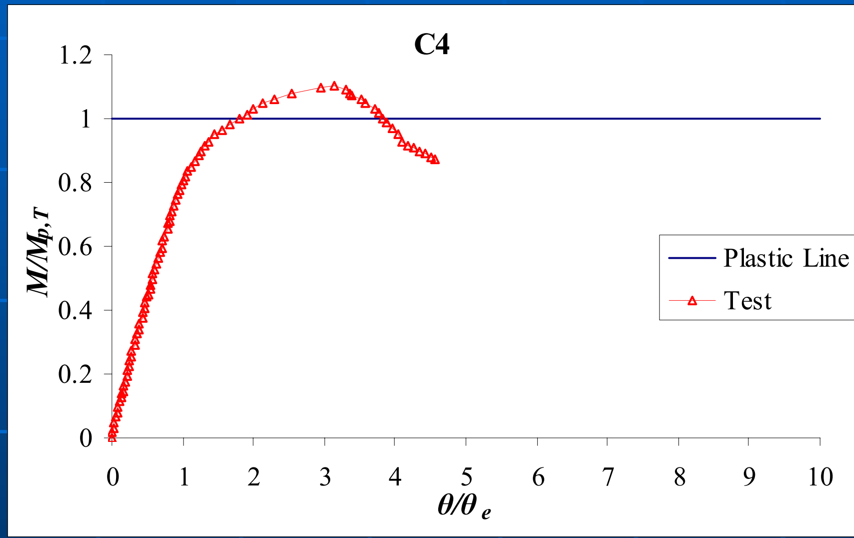

- No local or global buckling was seen on FEM before the plastic moment capacity was reached
- A gradual load reduction occurred without sudden failure
- Failure mode - mainly local buckling near mid-span

Experimental Investigation on Composite Beams

- General Observations

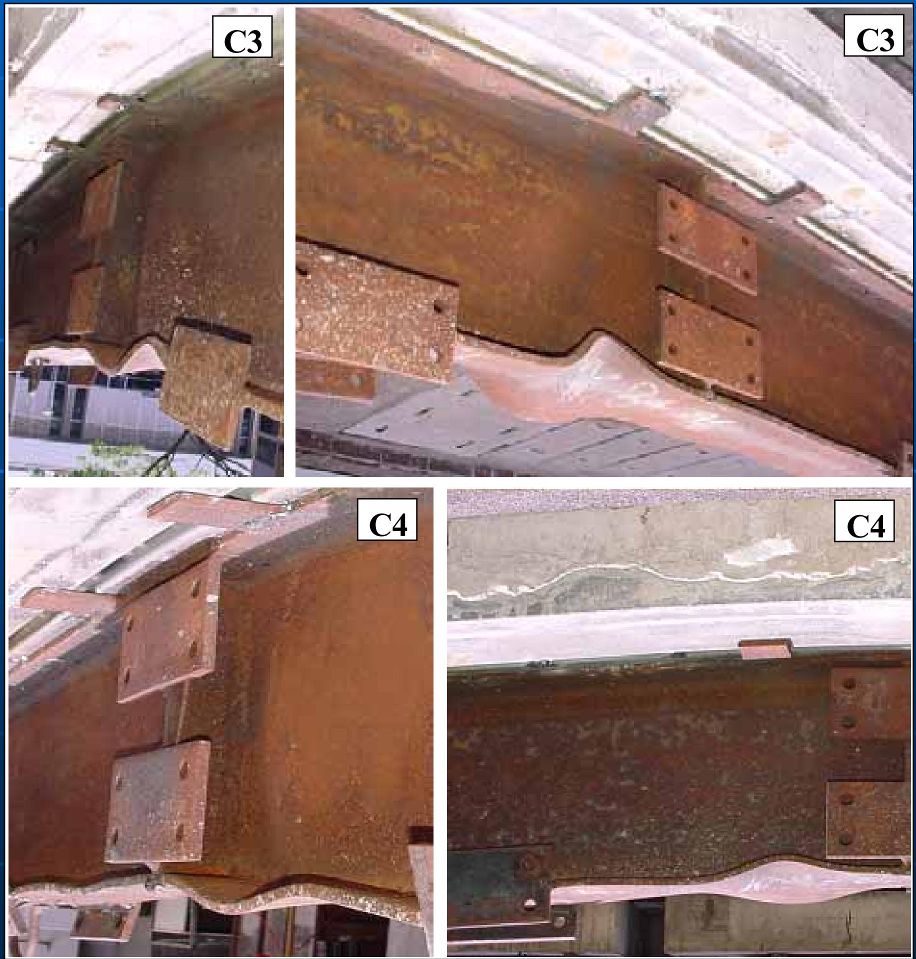

- ➢Anti-symmetric local buckling of bottom flange where one side of flange curled up while the other side twisted downwards
- ➢Local buckling of web occurred at almost the full depth of the web
- ➢Local buckling failure occurred on only one half of the beam

Experimental Investigation on Composite Beams

- Key Findings & Discussions

➢The main component of composite beam is the primary reinforcement

➢Plastic neutral axis located within the top flange, or near to the web-top flange junction

➢Degree of shear connection was not reduced even when the beam was heated, since the temperature of shear stud was below 300° C

➢An increase in ultimate moment capacity for C2 due to misalignment of beam during test set-up; protection material was skewed to one side

➢Effects of flange and web slenderness, effective length, degree of shear connection and reinforcement ratio cannot be quantified from the test results since only four tests had been conducted and the temperature distribution for each test was different

Experimental Investigation on Composite Beams

- Key Findings & Discussions

Temperature distribution across the section of a composite beam is proposed

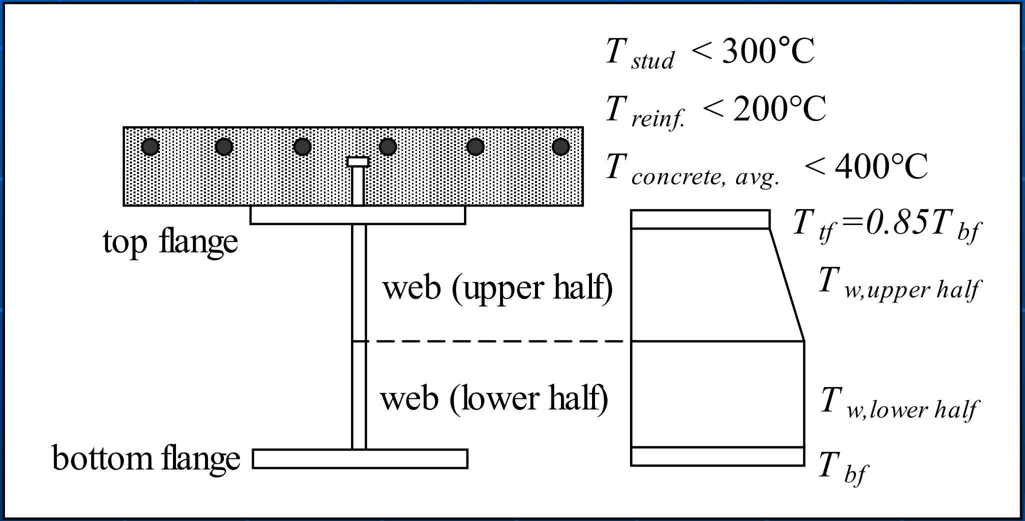

- Temperature of bottom half of web assumed constant and equal to bottom flange temperature
- Temperature of upper half of web assumed to vary linearly from T_{bf} to $0.85T_{bf}$ at the web-top flange junction
- Temperature of concrete, shear stud and reinforcement assumed to be less than 400° C, 300° C and 200° C

Experimental Investigation on Composite Beams

- Key Findings & Discussions

Comparisons of failure modes with Cardington test

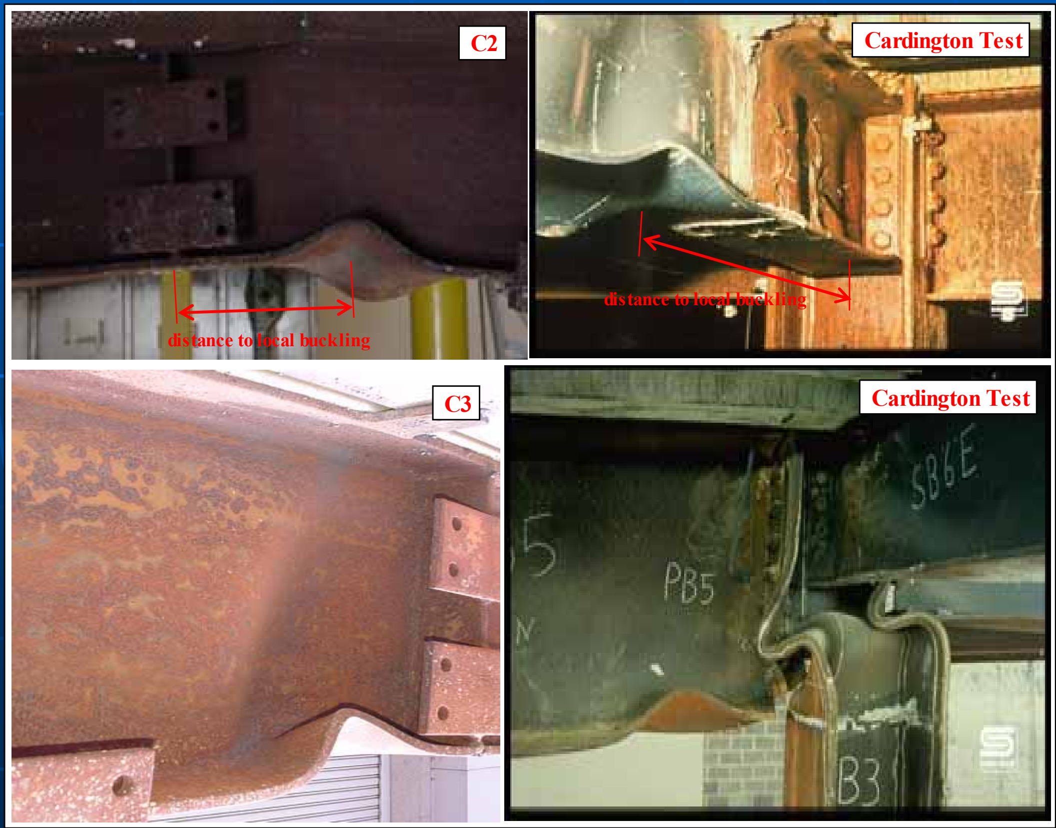

Experimental Investigation on Composite Beams

- Comparison With Steel Beam Test

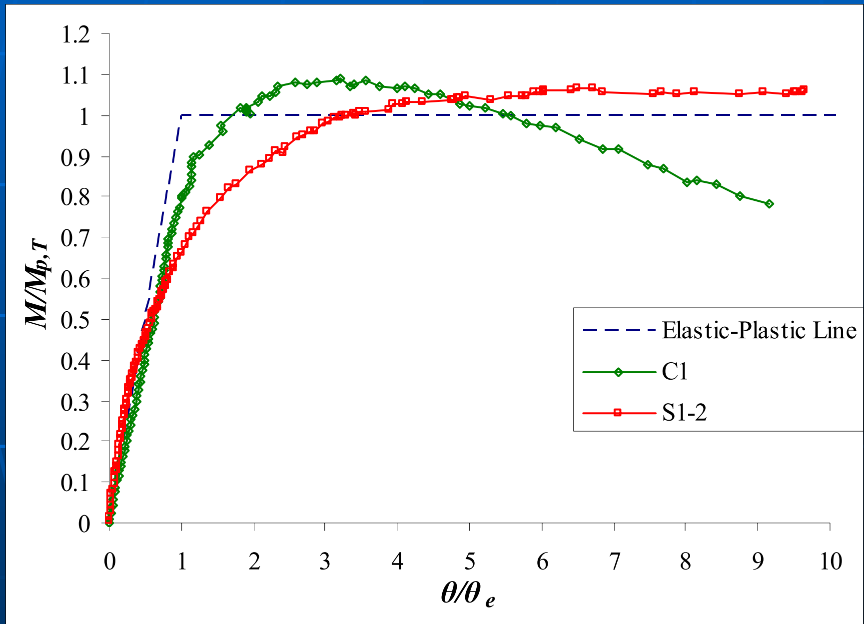

- C1 reached its plastic moment capacity at a much lower rotation
- Ultimate rotation for C1 was much lower
- Moment-rotation response of C1 was less non-linear
- Loss of ductility in the composite beam due to increased depth of web in compression caused by shifting of neutral axis towards the top flange

Test No.	$T_{bot.\ flange}$ (°C)	L_E (mm)	$M_{p,T}$ (kNm)	M_m (kNm)	$M_m/M_{p,T}$	θ_p/θ_e	θ_u/θ_e	r_a
S1-2	615	650	102.85	109.62	1.066	3.389	13.169*	2.81*
C1	623	563	133.89	146.05	1.091	1.783	5.544	2.11

*estimated from numerical result

Finite Element Analysis (Steel)

- Overview
  - Four node rectangular thick shell element from MSC.MARC Mentat
  - Geometrical and material nonlinearities
  - Arc-length approach
  - Von Mises yield criterion
  - Initial imperfection in the form of a half sine curve
  - Validate FEM with Lukey and Adams tests (1969)

Finite Element Analysis (Steel)

- Validation (Ambient Temperature)

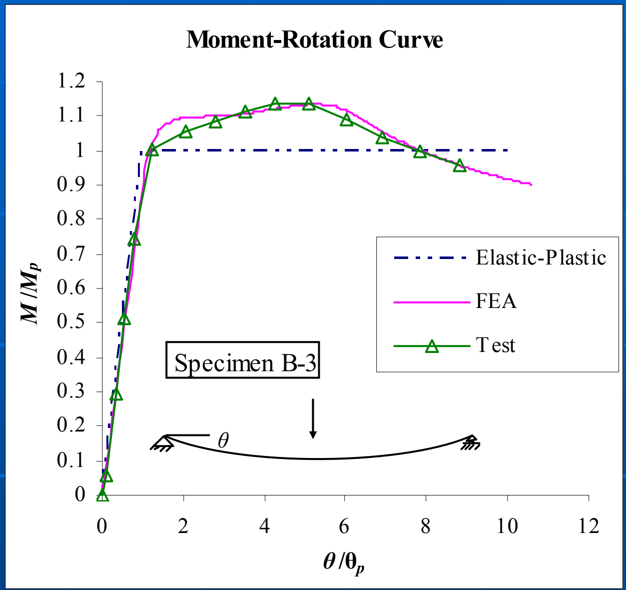

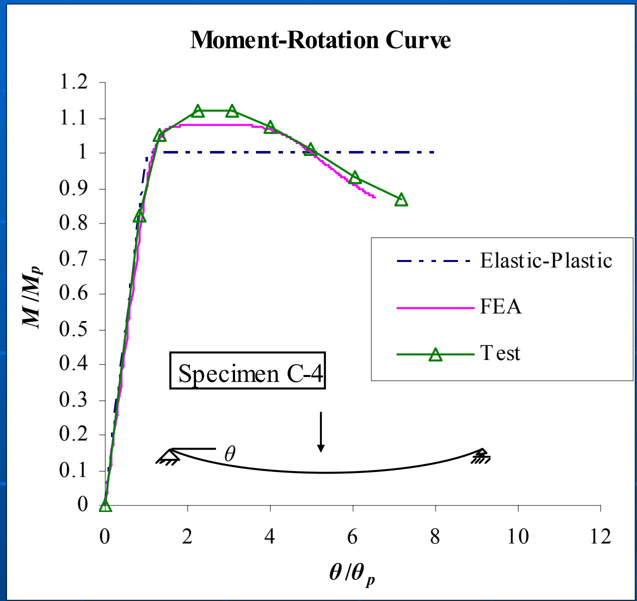

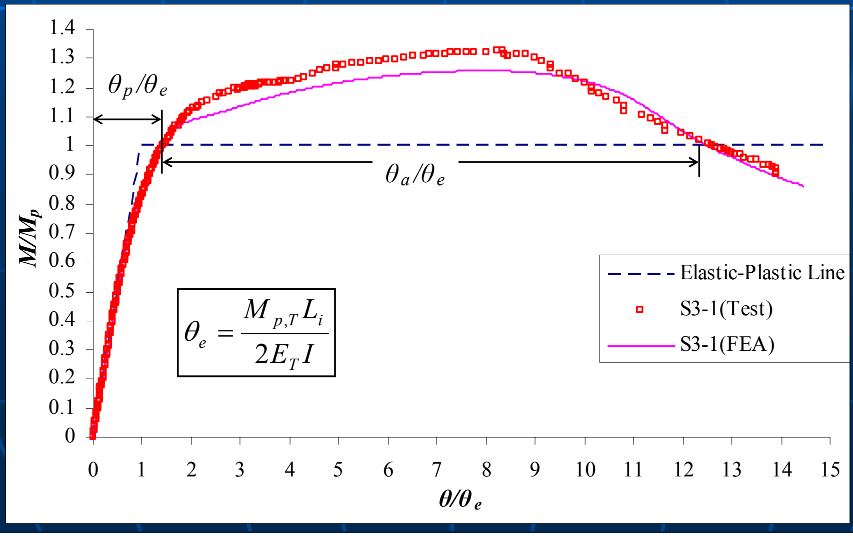

Finite Element Analysis (Steel)

- Validation (Elevated Temperature)

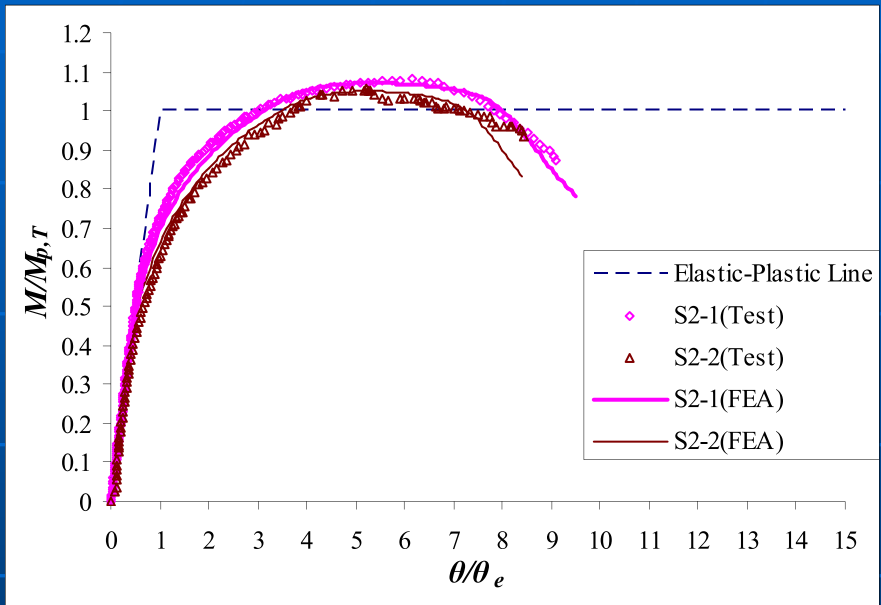

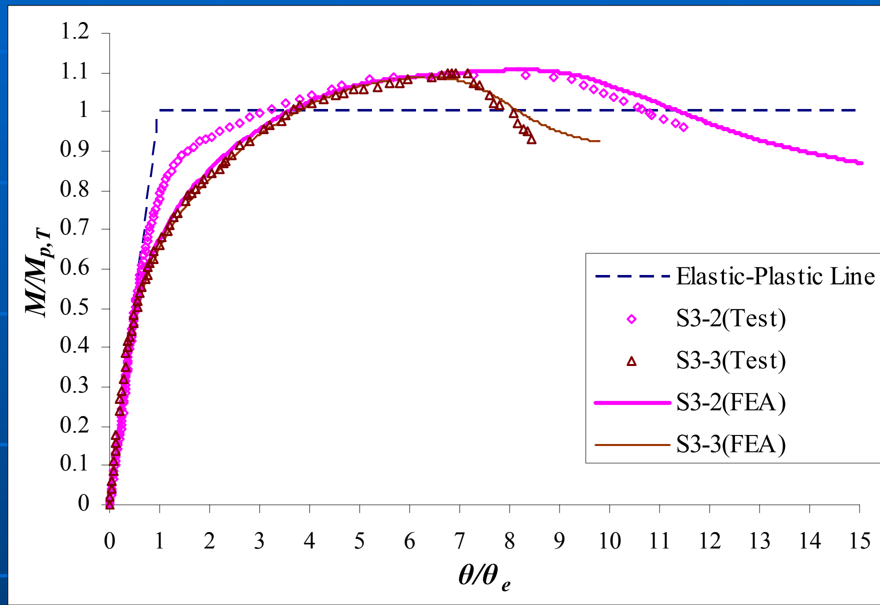

➢ Predictions of maximum moments within 2%

➢ Excellent agreement between test results and FE predictions due to accuracy of initial imperfection

➢ Slight discrepancy in response may be attributed to the differences between the stress-strain relationships proposed by EC3:1.2 and the actual stress-strain relationship

Finite Element Analysis (Steel)

- Parametric Study (Temperature)

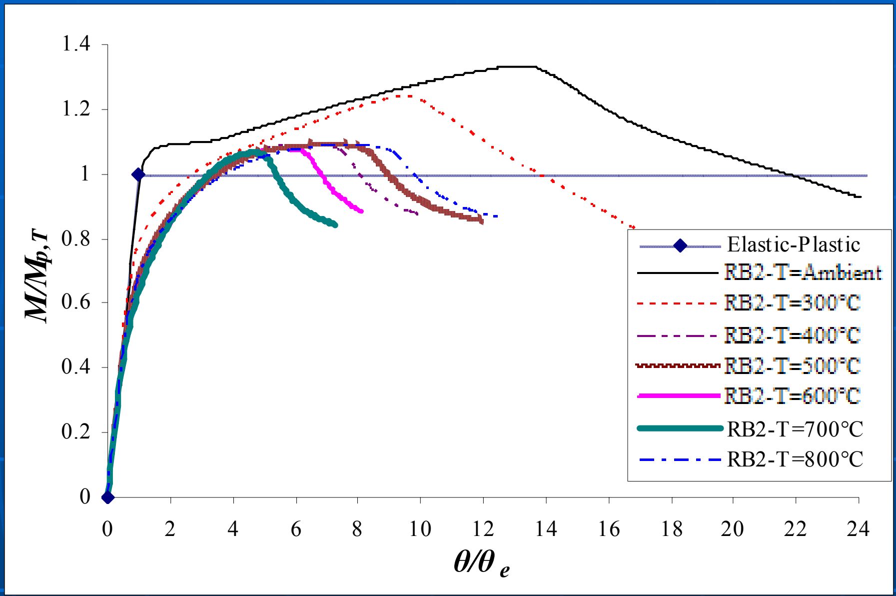

- Rotational capacity reduces as temperature increases
- Compare the trend of rotational capacity with the ratio of elastic modulus to yield strength at elevated temperature

$$E_T / f_{yT} = k_E E / k_y f_y$$

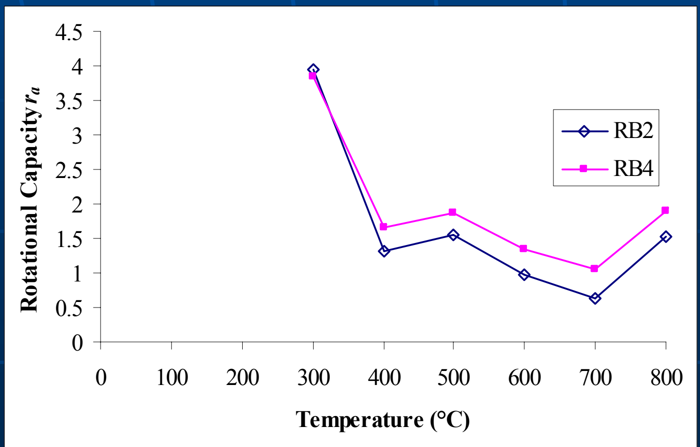

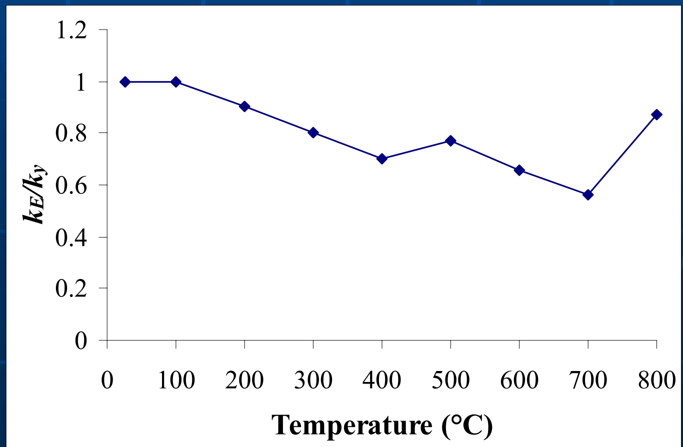

Finite Element Analysis (Steel)

- Parametric Study (Effective Length)

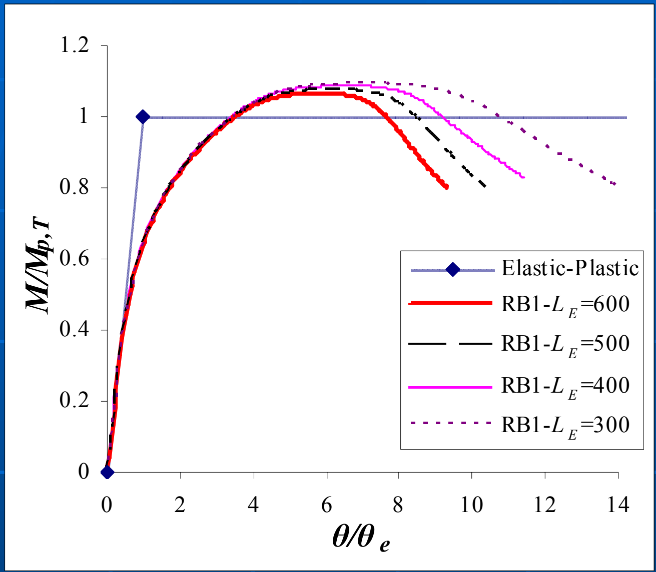

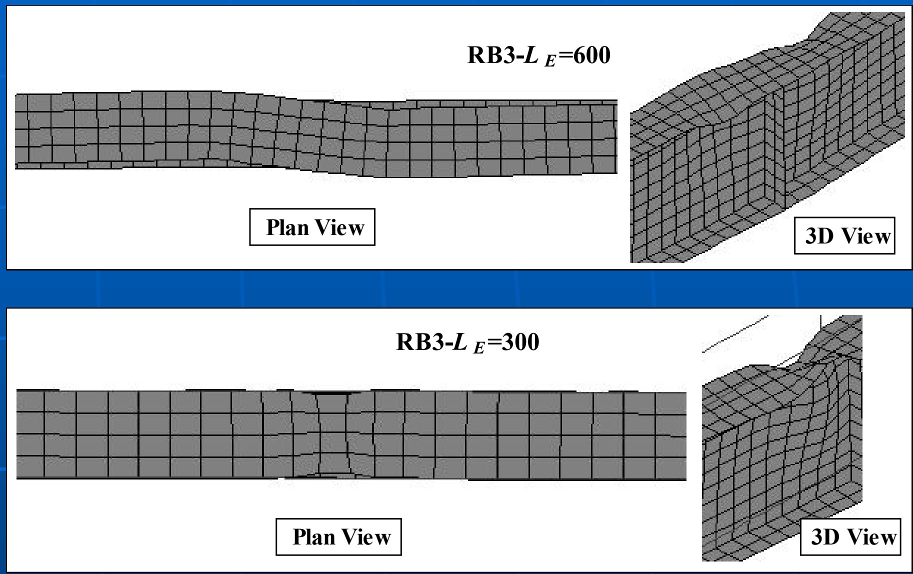

- Reducing the effective length increases both the maximum moment and rotational capacity
- A change of failure modes when effective length is reduced
- Improvement to the rotational capacity can be achieved by reducing the effective length for beams in which global buckling mode is observed

FE Analysis (Composite)

- Overview
  - Structural steel - four node rectangular thick shell element
  - Concrete slab - 20-node iso-parametric solid element
  - Reinforcement - iso-parametric, three-dimensional, 20-node solid element
  - Adjacent top flange and concrete nodes tied together using rigid links in two global displacements
  - The relative slip in *x*-direction between the steel beam and concrete element is governed by the load-slip relationship of shear stud connectors, and is simulated using linear springs
  - Uniaxial representation of constitutive law in terms of true stress and logarithmic strain

FE Analysis (Composite)

- Validation

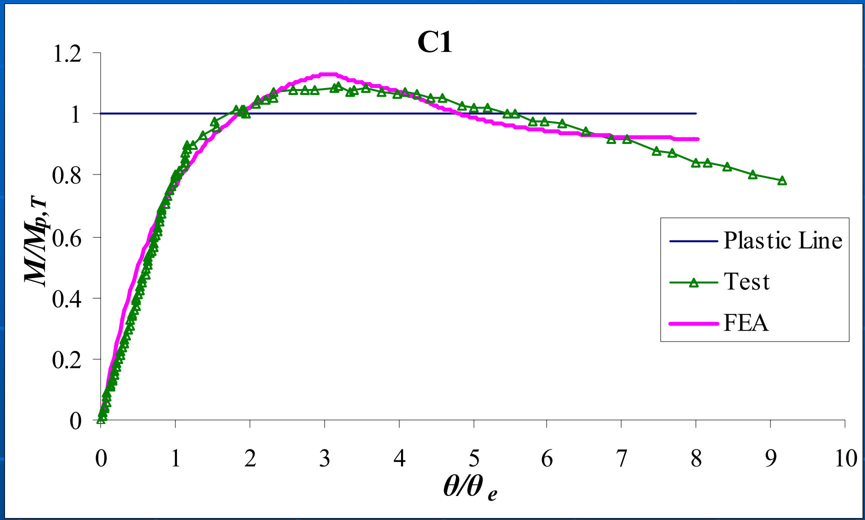

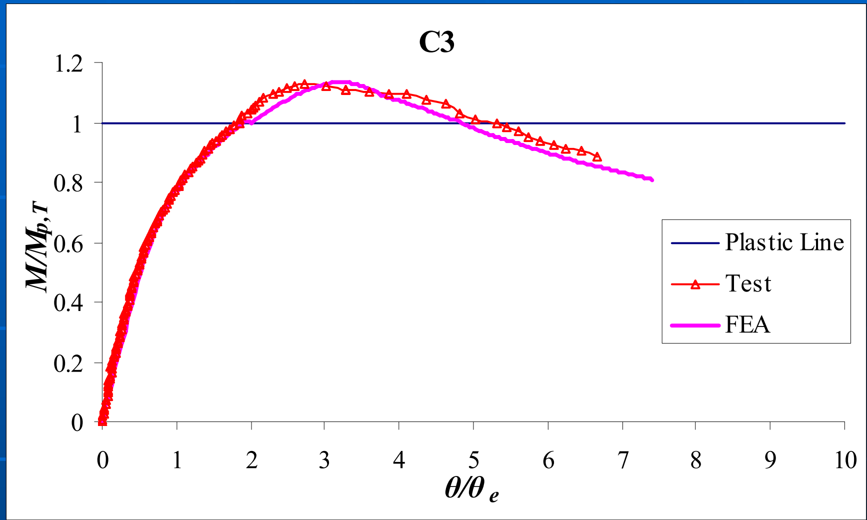

Test	Citical Temperature Distribution (°C)						$M_m/M_{p,T}$		r_a	
No.	$flange_{bot}$	web	$flange_{top}$	rebar	concrete	stud	Test	FEA	Test	FEA
C1	623	634	560	113	222	320	1.091	1.129	2.11	1.60
C2	601	603	520	103	144	250	1.183	1.107	1.84	1.10
C3	515	512	427	104	169	188	1.130	1.134	1.85	1.52
C4	542	538	463	121	238	260	1.103	1.115	1.00	0.87

FE Analysis (Composite)

- Validation

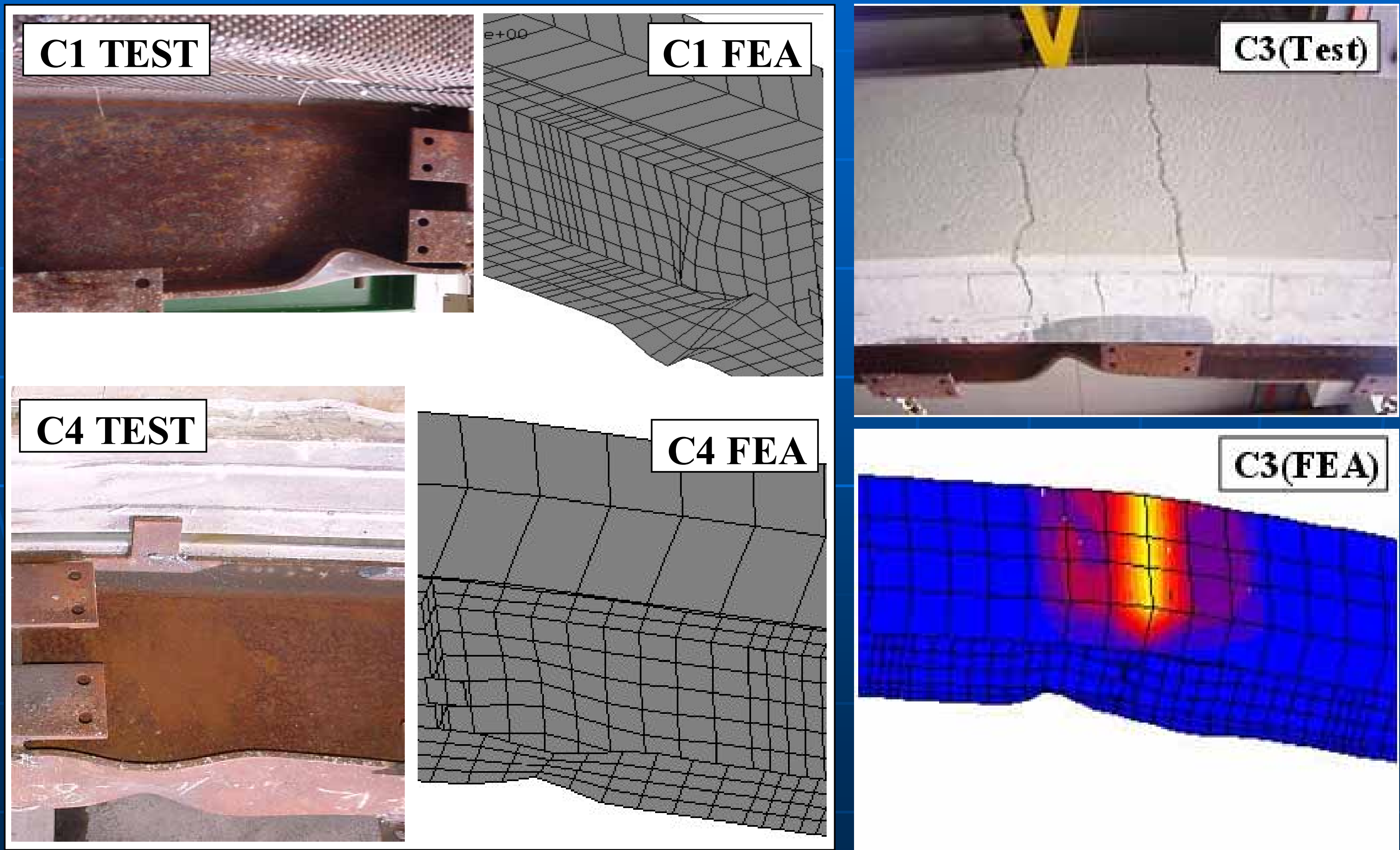

FE Analysis (Composite)

- Parametric Study (Temperature)

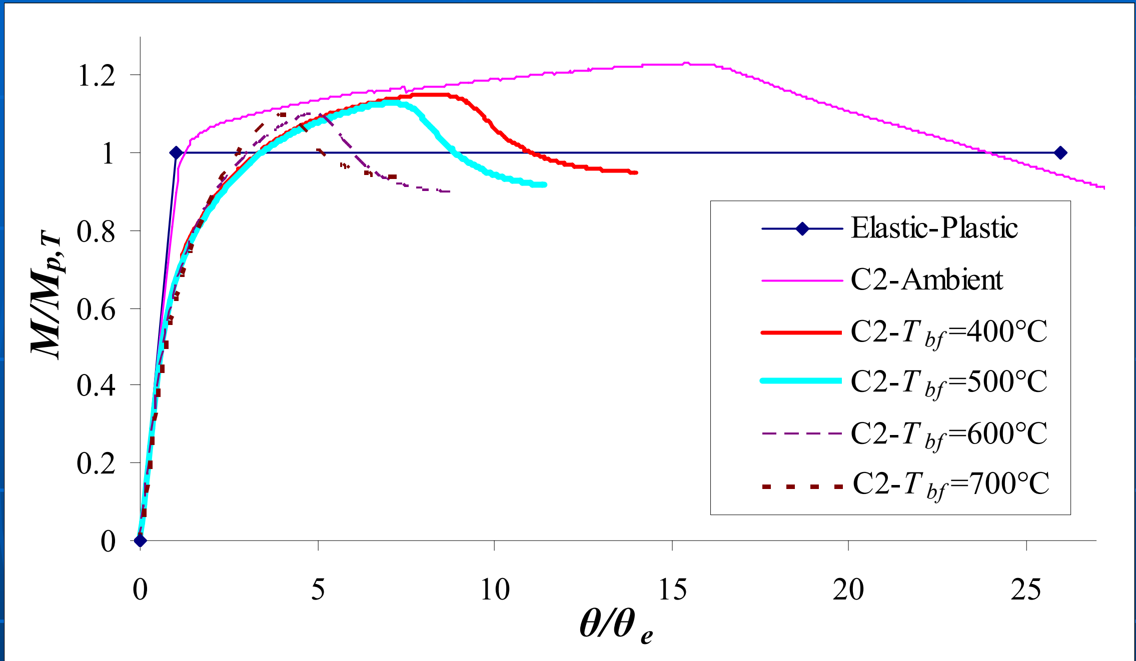

➢Proposed temperature distributions is used

➢As temperature increases, rotational capacity reduces. This trend is different from that of steel beams because the strength and stiffness of the compression and tension parts of composite beams do not reduce at the same rate

➢At ambient temperature, the beam possesses large inelastic rotation due to a very low plastic rotation and a large ultimate rotation. The presence of strain hardening at ambient temperature also helps to delay the local buckling of flange and web, hence increasing the ductility tremendously.

Modelling of Moment-Rotation

- Steel Beams

Moment-Rotational Relationship is divided into 3 parts

- Non-Linear Pre-Peak
- Horizontal Plateau
- Unloading Region

- Non-Linear Pre-Peak Region

- Rotation θ can be obtained from the integration of the curvature diagram:

$$\theta = \int_0^x \chi(x) \quad dx$$

- Discretization of the cross-section into small elementary areas and dividing the longitudinal length into smaller sections is needed since the stress-strain relationship of steel at elevated temperature is non-linear

Modelling of Moment-Rotation

- Steel Beams

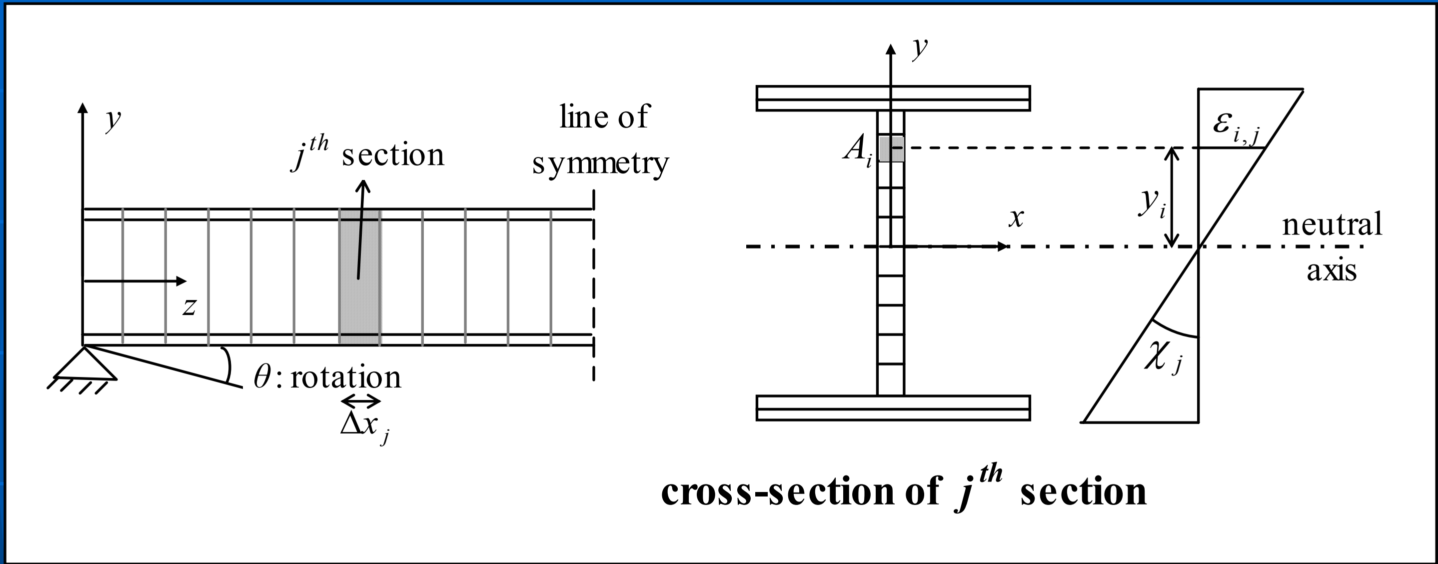

➢At a certain load, bending moment at j^{th} section is calculated

➢Curvature at j^{th} section evaluated using both compatibility and equilibrium equations

$$\varepsilon_{i,j} = \chi_j y_i \qquad \sum_{i=1}^{n} \sigma_i A_i y_i = M_j$$

➢Rotation can be calculated from:

$$\theta = \sum_{j=1}^{m} \chi_j \Delta x_j$$

Modelling of Moment-Rotation

- Steel Beams
  - Horizontal Plateau Region

    ➢Since the maximum moment achieved for steel beams with temperature exceeding 400° C is generally less than 10% above their plastic moment capacity, it is sufficient to use a horizontal line at the plastic moment capacity to connect the non-linear pre-peak curve with the unloading curve

    ➢Horizontal line will begin at plastic rotation θ_p up to ultimate rotation θ_u, in which the unloading curve crosses the plastic moment capacity

  - Unloading Region (Statistical Approach)

    ➢Both the ultimate rotation θ_u, which determines the start of unloading curve, and the unloading moment-rotation equation need to be determined

    ➢A multi-linear regression model is used to predict the ultimate rotation

    ➢a quadratic equation with coefficients obtained from the regression of FE's post-buckling curves is used to describe the unloading moment-rotational relationship

Modelling of Moment-Rotation

- Steel Beams
  - Unloading Region
    - The best regression model to predict the ultimate rotation:

$$\sqrt{\frac{\theta_u}{\theta_e}} = 8.21 - 1.26\frac{k_y}{k_E} - 0.14\sqrt{\frac{c}{t_f}\gamma_f}\sqrt{\frac{d}{t_w}\gamma_w} - 0.0518\lambda_{LT} \geq \sqrt{\frac{\theta_p}{\theta_e}}$$

Recommended range of use

$4.0 \leq c/t_f \leq 13.0$ $\quad 24.0 \leq d/t_w \leq 81.0$ $\quad 11.0 \leq \lambda_{LT} \leq 29.0$

$400^o C \leq T \leq 800^o C$ $\quad 355\ MPa \leq f_y \leq 275\ MPa$

- The unloading moment-rotation equation is defined as

$$\frac{M}{M_{p,T}} = 1 - 0.12\left(\frac{\theta}{\theta_e} - \frac{\theta_u}{\theta_e}\right) + 0.023\left(\frac{\theta}{\theta_e} - \frac{\theta_u}{\theta_e}\right)^2$$

in which $\theta_u/\theta_e \leq \theta/\theta_e \leq \theta_u/\theta_e + 2$

Modelling of Moment-Rotation

- Steel Beams
  - Validation of Design Model

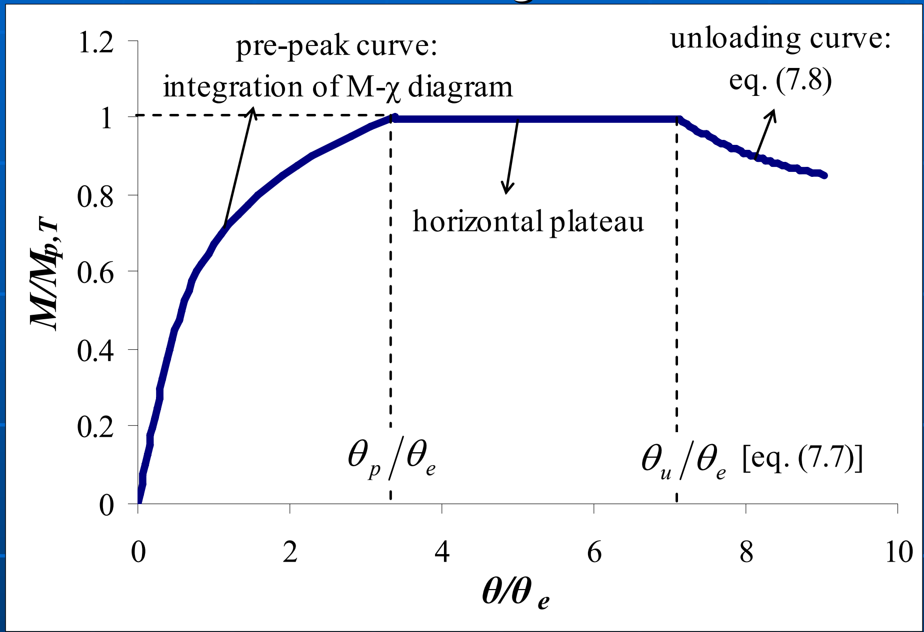

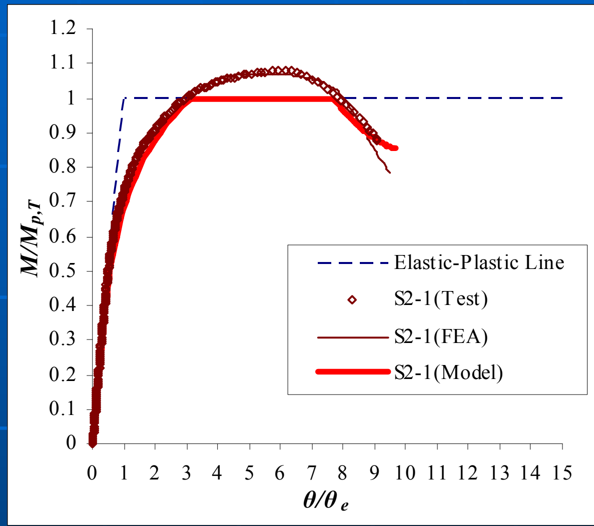

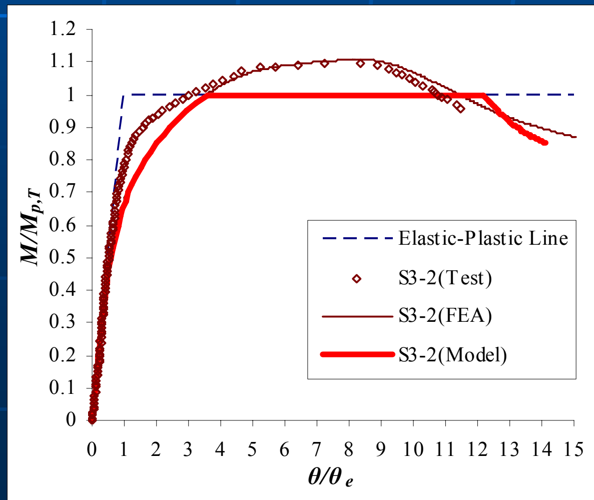

Modelling of Moment-Rotation

- Steel Beams
  - Unloading Region (Plastic Collapse Mechanism Approach)
    - ➢Based on upper bound theorem to plot the post-critical curve
    - ➢Very useful to determine the ultimate plastic rotation and the available rotational capacity

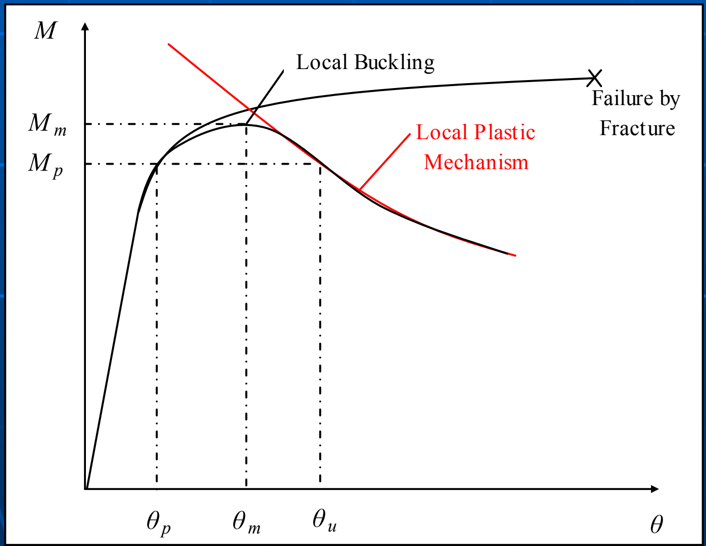

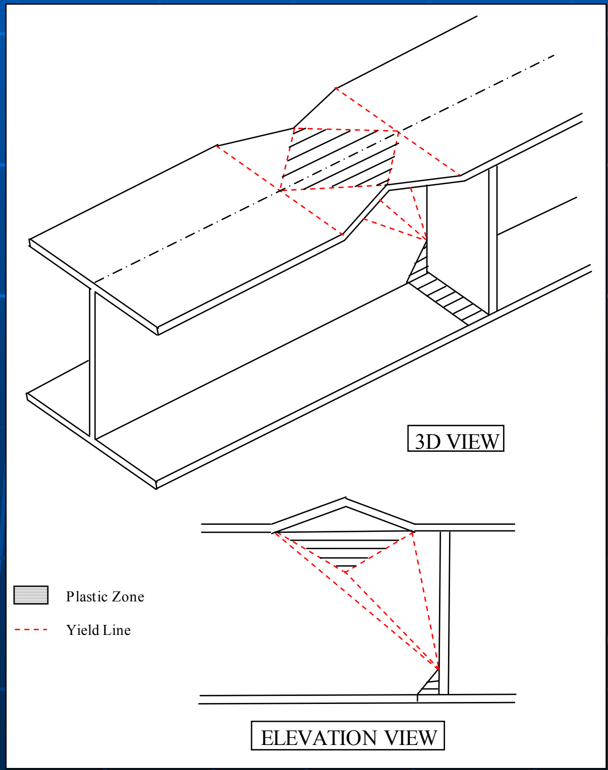

Modelling of Moment-Rotation

- Steel Beams
  - Unloading Region (Plastic Collapse Mechanism Approach)

➢Many different models available for steel beams at ambient temperature. The model by Gioncu & Petcu (2001) is extended to elevated temperature in this research

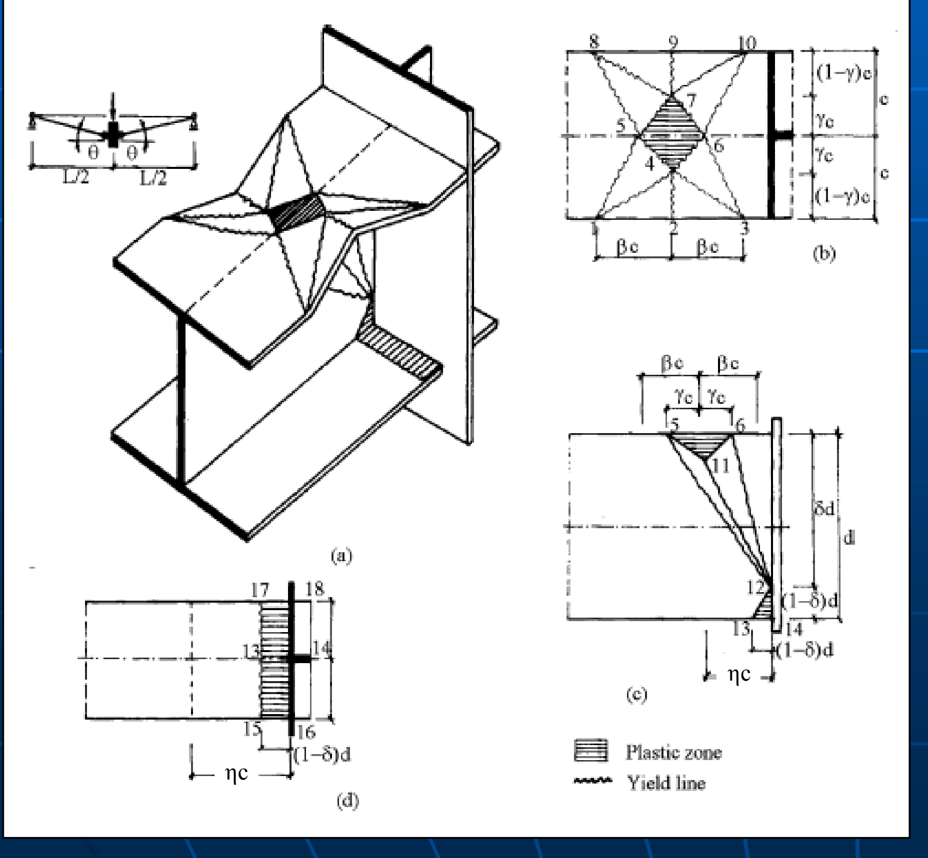

✓Buckled shape of the compression flange is represented by a double-triangular plastic zone and several yield lines

✓Buckled shape of the web is represented by an upper triangular plastic zone connected by several yield lines to the centre of rotation “12”

✓As rotation occurs, the tension zone remains in plane and experiences simple tensile inelastic deformation

Modelling of Moment-Rotation

- Steel Beams
  - Unloading Region (Plastic Collapse Mechanism Approach)

At point of collapse (local plastic mechanism is formed), the total external virtual work done:

$$W_{ext} = \sum P_i \Delta_i$$

The total internal virtual work of the mechanism:

$$W_{\text{int}} = \sum_i (W_l)_i + \sum_j (W_z)_j$$

in which,

$$W_l = \frac{t^2 p_y}{4} \int_{l_p} f(\theta) dl \longrightarrow W_l = \frac{l_p t^2}{4} p_y \theta$$

$$W_z = t p_y \int_{A_p} f(\varepsilon) dA \longrightarrow W_z = A_p t p_y \varepsilon$$

Modelling of Moment-Rotation

- Steel Beams
  - Unloading Region (Plastic Collapse Mechanism Approach)

Thus, the total internal virtual work mechanism:

$$W_{\text{int}} = \frac{1}{4}\sum_i (l_p t p_y \theta)_i + \sum_j (A_p t p_y \varepsilon)_j$$

Finally, equating the internal and external works done:

$$M = \frac{W_{\text{int}}}{\theta}$$

Modelling of Moment-Rotation

- Steel Beams
  - Unloading Region (Plastic Collapse Mechanism Approach)

Extension of the model to elevated temperature:

✓Length of mechanism slightly reduced at elevated temperature because of the disappearance of strain-hardening phenomenon which limits the spread of plasticity

✓Parameter β which determines the length of mechanism modified as

$$\beta_T = 0.713 \boxed{\sqrt{\frac{275}{f_{yf,c}}}} \left(\frac{d}{b}\right)^{1/4} \left(\frac{t_f}{t_w}\right)^{3/4} \boxed{\left(\frac{k_E / k_y}{0.7}\right)}$$

modifies the material coefficient of 0.713 and indicates that, as the steel grade increases the length of mechanism is reduced, which is in line with experimental and numerical evidence

take into account the effect of temperature on the unloading curve and rotational capacity

Modelling of Moment-Rotation

- Steel Beams
  - Validation

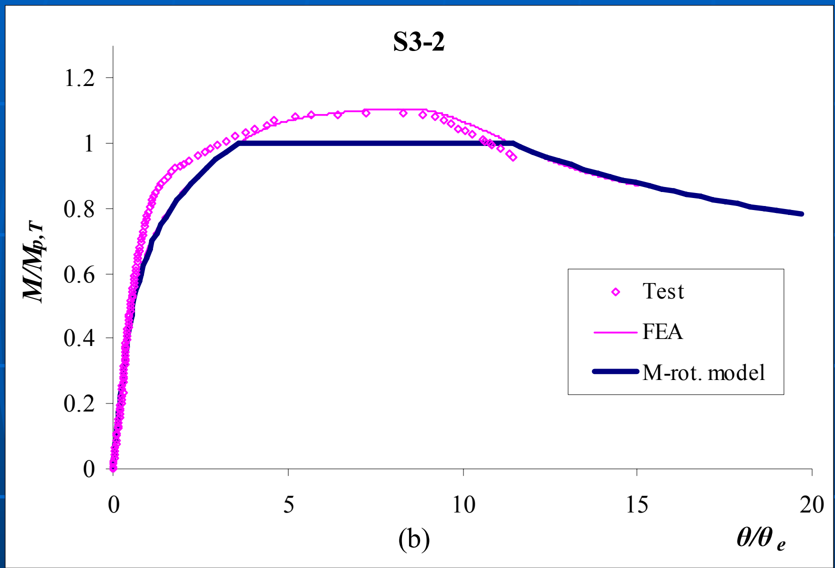

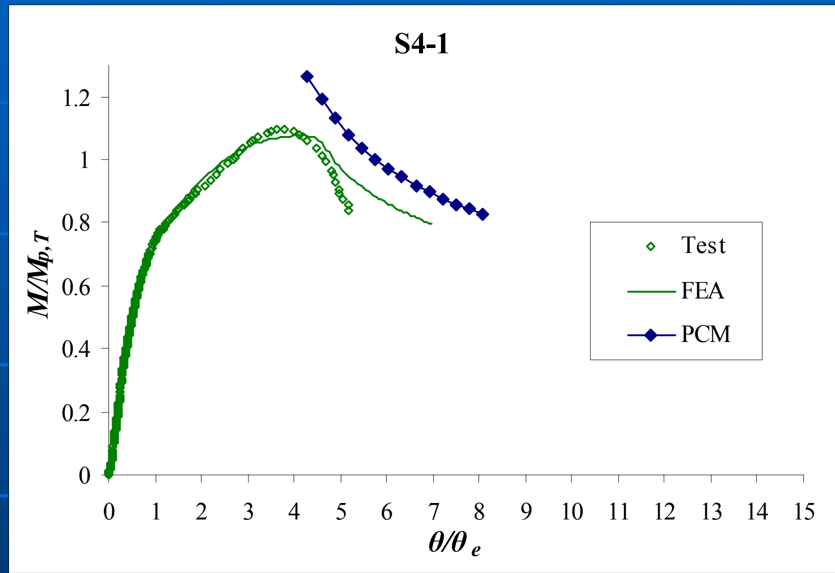

✓PCM method is best used within the limits of parameters:

$$4.0 \le (c/t_f)\gamma_f \le 10.0 \qquad 24.0 \le (d/t_w)\gamma_w \le 44.0 \qquad 11.0 \le \lambda_{LT} \le 20.0$$

$$\left((d/t_w)\gamma_w \big/ (c/t_f)\gamma_f\right) \le 5.5 \qquad 400^o C \le T \le 800^o C$$

Modelling of Moment-Rotation

- Composite Beams
  - The pre-peak region before buckling can be evaluated the same way as steel beams
  - Unloading Region (Plastic Collapse Mechanism Approach)

✓One additional internal work done by the plastic zone of the reinforcement has to included

✓This internal work done by the reinforcement can be calculated by integrating the strain energy over the deforming volume (plastic zone):

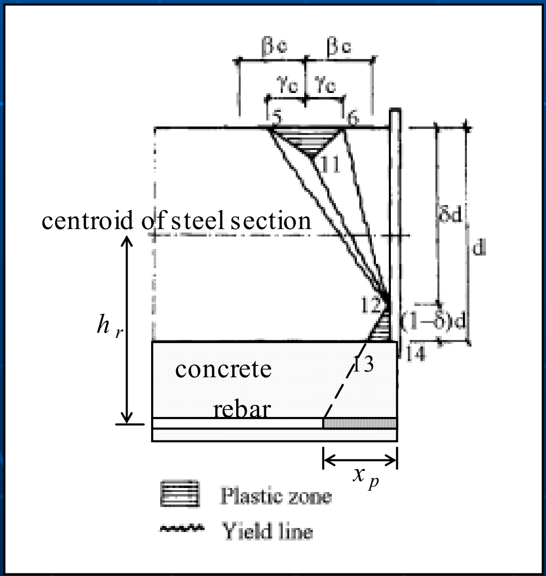

$$W_{int}^{reinf} = A_s x_p f_{yr,T} \theta$$

Modelling of Moment-Rotation

- Composite Beams
  - Unloading Region (Plastic Collapse Mechanism Approach)

✓An empirical factor to take into account the increased portion of the web in compression is added to the length of mechanism

$$\beta_T^{comp} = 0.713 k_w \sqrt{\frac{275}{f_{yf,c}}} \left(\frac{d}{b_f}\right)^{1/4} \left(\frac{t_f}{t_w}\right)^{3/4} \left(\frac{k_E / k_y}{0.7}\right)$$

in which, $k_w = 0.5d \big/ \alpha d$ and α is the portion of the web in compression

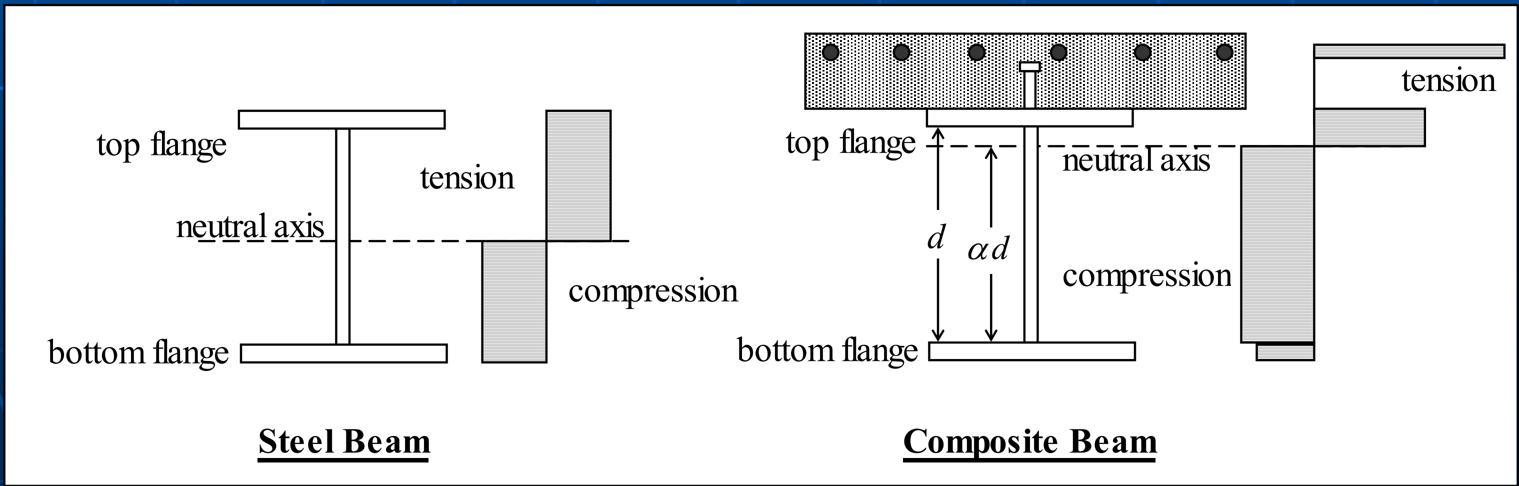

Modelling of Moment-Rotation

- Composite Beams
  - Validation

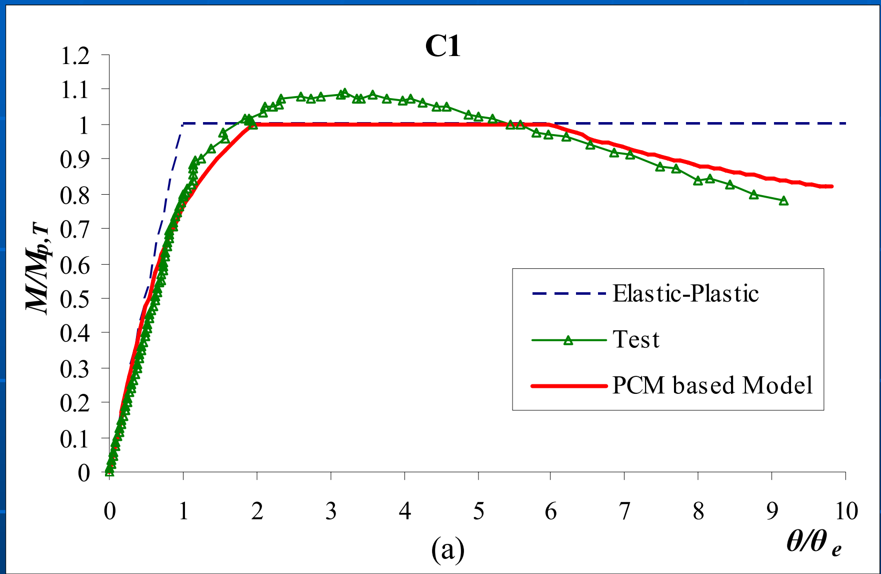

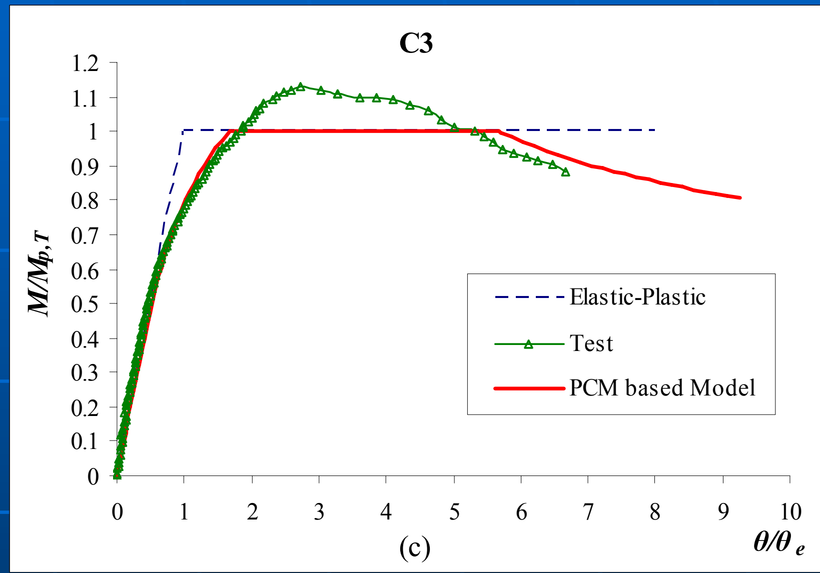

Test No.	θ_u/θ_e		r_a		$\frac{(\theta_u)_{PCM}}{(\theta_u)_{Test}}$
	Test	PCM	Test	PCM	
C1	5.544	5.971	2.11	2.05	1.077
C2	5.879	6.565	1.84	2.49	1.117
C3	5.306	5.674	1.85	2.39	1.069
C4	3.829	4.272	1.00	1.38	1.116

Conclusions

- The ductility issue of both steel and composite beams in the hogging moment regions under fire conditions has been highlighted by 4 composite beam specimens
- Extensive numerical analysis to identify key factors affecting the local buckling and the failure patterns
- Propose a moment-rotational relationship for both steel and composite beams subjected to hogging moment at elevated temperatures
- The proposed moment-rotation design model comprises three parts: a non-linear pre-peak curve, a horizontal plateau at the plastic moment capacity and an unloading curve

Recommendations

- Additional tests on composite beams to includes beams with partial shear connections or other types of decking and shear connectors
- Study the moment-rotational relationship of the inner span of continuous beam under hogging moment, that is, thermal restraint is present
- Behaviour of steel and composite frames related to redistribution of moment during fire be studied using proposed moment-rotational relationship to incorporate the local buckling effect
- Study the behaviour of composite beams with the joints under elevated temperatures

THANK YOU

Q&A SESSION

List of Publications

1. Dharma, R. B. and Tan, K. H. (2005), "Alternative Approach for Lateral Torsional Buckling of Unrestrained Beams in Fire", <u>Proceedings of the Fourth International Conference on Advances in Steel Structures</u>, Shanghai, Elsevier Ltd., pp.949-957.
2. Dharma, R. B. and Tan, K. H. (2005), "A Numerical Study of Rotational Capacity of Steel Beams in Fire", <u>Proceedings of the Fourth International Conference on Advances in Steel Structures</u>, Shanghai, Elsevier Ltd., pp.981-989.
3. Dharma, R. B. and Tan, K. H. (2006), "Ductility of Steel and Composite Beams under Fire Conditions", <u>Proceedings of the International Symposium on Advances in Steel and Composite Structures</u>, Singapore, CACS, pp. 84-99.
4. Dharma, R. B. and Tan, K. H. (2006), "Proposed Design Methods for Lateral Torsional Buckling of Unrestrained Steel Beams in Fire", accepted for publication in <u>Journal of Constructional Steel Research</u>.

List of Publications

5. Dharma, R. B. and Tan, K. H. (2006), "Rotational Capacity of Steel I-Beams under Fire Conditions, Part I: Experimental Study", accepted for publication in <u>Engineering Structures</u>.
6. Dharma, R. B. and Tan, K. H. (2006), "Rotational Capacity of Steel I-Beams under Fire Conditions, Part II: Numerical Simulations", accepted for publication in <u>Engineering Structures</u>.
7. Dharma, R. B. and Tan, K. H. (2006), "Experimental and Numerical Investigation on Ductility of Composite Beams in the Hogging Moment Regions under Fire Conditions", submitted for publication in <u>ASCE Journal of Structural Engineering</u>.

Literature Review of Steel Properties

- Stress-Strain Relationship

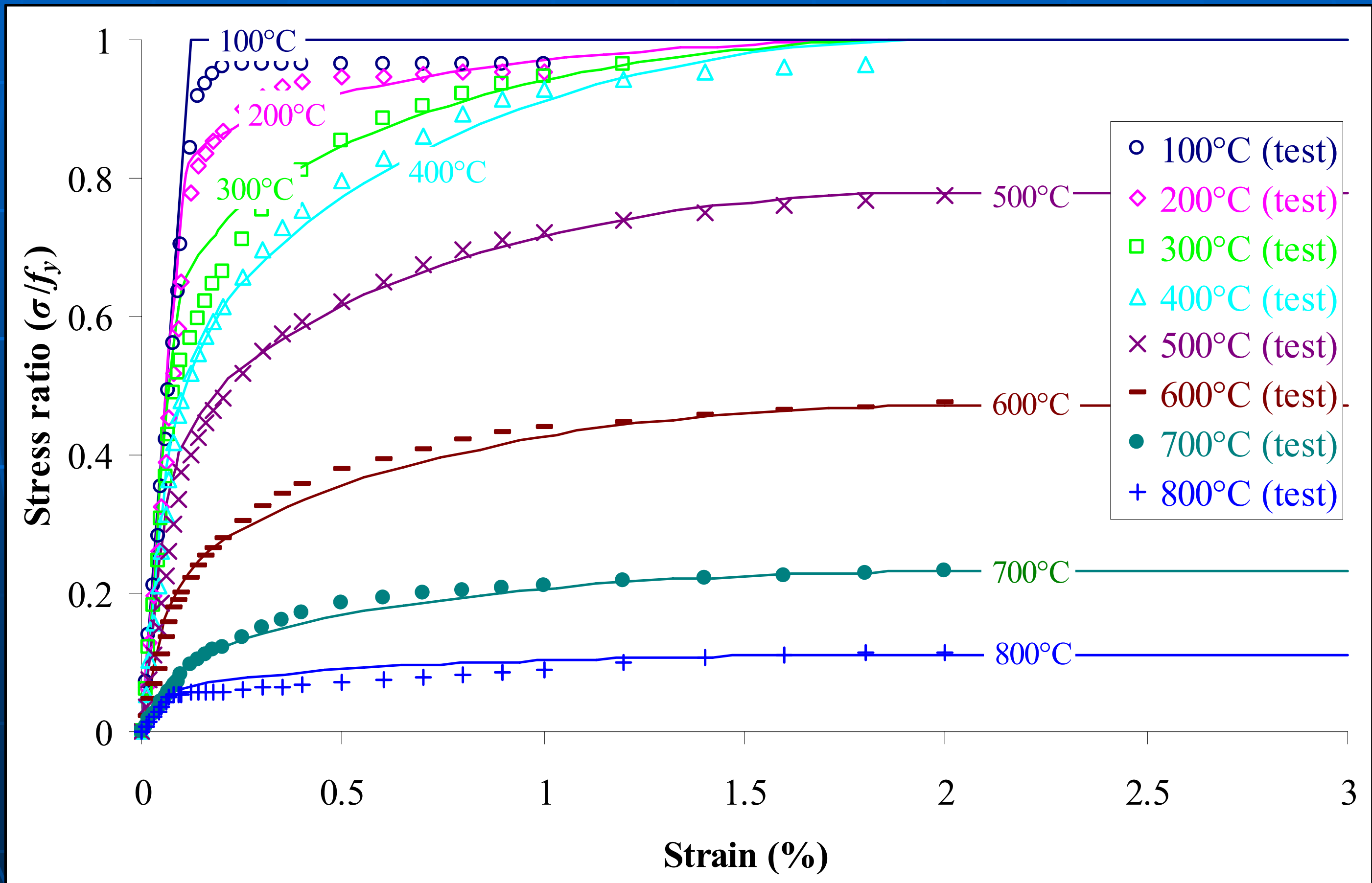

Literature Review of Load-Slip Relationship of Shear Stud

Based on Zhao & Kruppa (1995) Model

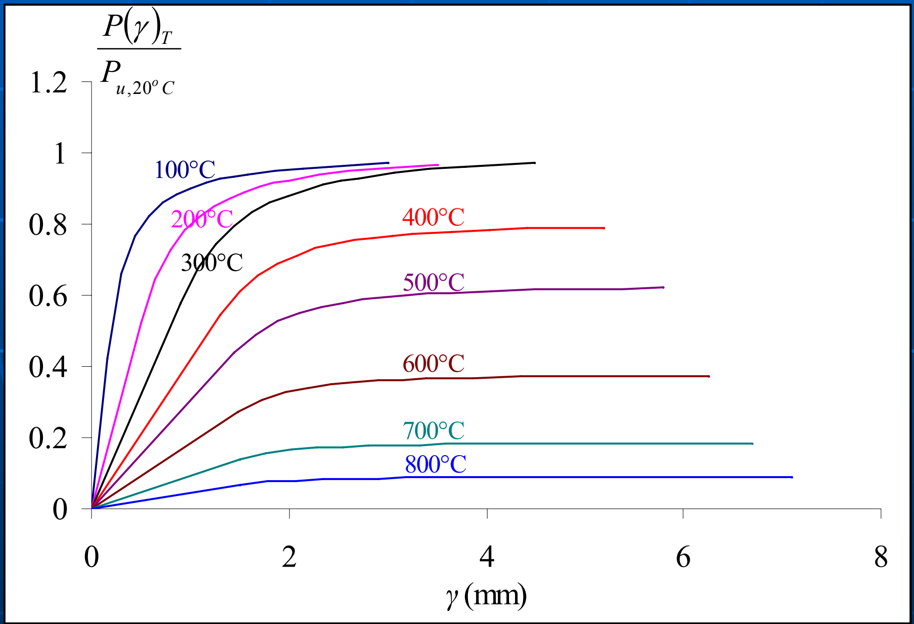

Temperature (°C)	$\frac{P_{u,T}}{P_{u,20^oC}}$	k	γ_o (mm)	γ_u (mm)	γ_{max} (mm)
100	1.000	0.42	0.16	3.00	11
200	1.000	0.52	0.50	3.50	12
300	1.000	0.58	0.90	4.50	13
400	0.800	0.68	1.30	5.20	14
500	0.624	0.70	1.45	5.80	15
600	0.376	0.72	1.48	6.25	16
700	0.184	0.74	1.50	6.70	17
800	0.088	0.75	1.50	7.10	18